Structural bifurcation analysis in chemical reaction networks

Takashi Okada, Je-Chiang Tsai, and Atsushi Mochizuki

Structural Bifurcation Analysis in Chemical Reaction Networks

Takashi Okada[1,2], Je-Chiang Tsai[3], and Atsushi Mochizuki[1,2,4,5]

[1] iTHEMS Program, RIKEN, Wako 351-0198, Japan.

[2] Theoretical Biology Laboratory,
RIKEN, Wako 351-0198, Japan

[3] Department of Mathematics,
National Tsing Hua University, Hsinchu 300, Taiwan

[4] Laboratory of Mathematical Biology,
Institute for Frontier Life and Medical Sciences,
Kyoto University, Kyoto 606-8507, JAPAN

[5] CREST, JST, Kawaguchi 332-0012, Japan. *

In living cells, chemical reactions form complex networks. Dynamics arising from such networks are the origins of biological functions. We propose a novel mathematical method to analyze bifurcation behaviors of network systems using its structure alone. Specifically, a whole network is decomposed into subnetworks, and for each of them, the bifurcation condition can be studied independently. Further, parameters inducing bifurcations and chemicals exhibiting bifurcations can be determined on the network. We illustrate our theory using hypothetical and real networks.

I.   INTRODUCTION

In living cells, many chemical reactions are connected, sharing their products and substrates and constructing a large network. Biological functions are believed to arise from network dynamics of chemical reactions. Many examples of chemical reaction networks in living cells are available in databases [1–3], which are the accumulation of experimental results in biochemistry. On the other hand, the dynamics resulting from such complex network systems are not understood sufficiently, because of their complexity and limited information of kinetics and parameters.

It is widely considered that biological functions are regulated by the modulation of amounts or activities of enzymes. One popular experimental approach to understand the dynamics of such systems is to examine their sensitivity: each enzyme mediating a reaction in the system is increased/decreased or knocked out separately, and then the responses in concentrations of chemicals or their fluxes are observed [4]. In the previous studies [5–7], we developed a mathematical method, which determines sensitivity of steady states of chemical reaction networks to perturbations of parameters (enzyme amount/activities in the case of metabolism) from network structures. The method is based on an augmented matrix $\mathbf{A}$ (see Eq. (4)), where the distribution of nonzero entries directly reflects network structures. One of the striking results is the *law of localization* [6]. A substructure (subset of chemicals and reactions) in a network satisfying a topological condition is called a *buffering structure* (Fig. 1(1), (2)), which has the property that perturbations of reaction rate parameters inside a buffering structure influence only concentrations and fluxes inside this structure, and the outside remains unchanged under the perturbations.

Another important aspect of biological systems is qualitative change (i.e. plasticity) of behaviors induced by enzyme modulations or external conditions. Mathematically, these plastic behaviors can be interpreted as bifurcation behaviors of chemical reaction systems. There are some examples of mathematical studies for small and specific biological systems, where the dynamics is phenomenologically modeled by simple ordinary differential equations [8]. However, it has been considered difficult to analyze bifurcation properties for large complex networks, because of their large number of variables and parameters. At the same time, bifurcation properties have been usually studied under the assumption of specific kinetics, despite our poor knowledge of the actual kinetics in living cells. In other words, it has been considered impossible to study bifurcation behaviors of large systems from network information alone.

In this paper, we establish a novel theoretical method to study steady-state bifurcations of chemical reaction systems from the network information (see Fig. 1). This is achieved by (i) proving an equivalence between the Jacobian matrix J of a reaction system and that of the augmented matrix $\mathbf{A}$; (ii) investigating the dependence of the entries of $\mathbf{A}$ on reaction rates; and (iii) showing the relation between the null vectors of the matrices J and $\mathbf{A}$. We call the method "structural bifurcation analysis (SBA)". SBA leads to three important conclusions: (i) Factorization: bifurcation behaviors in a complex network can be studied by decomposing it into smaller subnetworks based on a topological condition on networks. For each subnetwork, the condition for bifurcation occurrence is determined from its structural information. (ii) Inducing parameters: for each subnetwork, bifurcation parameters are identifiable on the network. (iii) Bifurcating chemicals: for each subnetwork, chemicals exhibiting bifurcation behaviors are identifiable on the network. We remark that our usage of "parameter" always means a parameter associated with a reaction rate.

SBA allows us to study bifurcation behaviors based

* E-mail address: takashi.okada@riken.jp

on network information, even for large systems, by decomposing the network into subnetworks. We apply our method to hypothetical and real reaction networks, and demonstrate practical usefulness to analyze complex systems.

II. REVIEW OF STRUCTURAL SENSITIVITY ANALYSIS

We label chemicals by m ($m = 1, \cdots, M$) and reactions by n ($n = 1, \cdots, N$), and consider a spatially homogeneous chemical reaction system consisting of the following reactions

$$\sum_{m=1}^{M} y_m^n X_m \to \sum_{m=1}^{M} \bar{y}_m^n X_m, \ n = 1, \ldots, N.$$

A state of the reaction system is specified by concentrations $x_m(t)$, and obeys the differential equations

$$\frac{dx_m}{dt} = \sum_{n=1}^{N} \nu_{mn} r_n(\boldsymbol{x}; k_n), \ m = 1, \ldots, M. \quad (1)$$

Here, the $M \times N$ matrix ν is called the stoichiometric matrix, defined as $\nu_{mn} = \bar{y}_m^n - y_m^n$. The reaction rate functions r_n depends on $\boldsymbol{x}$ and also on rate parameters k_n. See (10) and (11) for an example.

To present the key idea, we assume that ν does not have nonzero cokernel vectors (see Supplemental Material for the general case [9]), implying that $\operatorname{rank}(\nu) = M \le N$ and the steady-state concentrations $\boldsymbol{x}^*$ and fluxes $\boldsymbol{r}^*$ are continuous functions of parameters $\{k_n\}_{n=1}^{N}$. In steady state, the flux $\boldsymbol{r}^*$ is expressed, in terms of the basis $\{\boldsymbol{c}_\alpha\}_{\alpha=1}^{N-M}$ of the kernel space of ν, as

$$\boldsymbol{r}^* = \sum_{\alpha=1}^{K} \mu^\alpha \boldsymbol{c}_\alpha, \quad K := N - M = \dim \ker \nu. \quad (2)$$

Now we review the *structural sensitivity analysis* [5] and the *law of localization* [6]. Under perturbation $k_{\hat{n}} \to k_{\hat{n}} + \delta k_{\hat{n}}$ ($\hat{n} = 1, \ldots, N$), the concentration changes $\delta_{\hat{n}} x_m$ and the flux changes $\delta_{\hat{n}} r_n$ at the steady state $\boldsymbol{x}^*$ are determined simultaneously by solving the following equation

$$\mathbf{A} \begin{pmatrix} \delta_1 \boldsymbol{x} & \ldots & \delta_N \boldsymbol{x} \\ \delta_1 \boldsymbol{\mu} & \ldots & \delta_N \boldsymbol{\mu} \end{pmatrix} = -\operatorname{diag}\left(\frac{\partial r_1}{\partial k_1} \delta k_1, \ \ldots, \ \frac{\partial r_N}{\partial k_N} \delta k_N \right), \quad (3)$$

where the horizontal line indicates structure of block matrices, $\delta_{\hat{n}} \boldsymbol{\mu} = (\delta_{\hat{n}} \mu^1, \ldots, \delta_{\hat{n}} \mu^K)^T$ is the change of the coefficients μ^α in (2) under the perturbation: $k_{\hat{n}} \to k_{\hat{n}} + \delta k_{\hat{n}}$, and the matrix $\mathbf{A}$ is given by

$$\mathbf{A} = \left(\frac{\partial \boldsymbol{r}}{\partial \boldsymbol{x}} \Big|_{\boldsymbol{x}=\boldsymbol{x}^*} - \boldsymbol{c}_1 \ldots - \boldsymbol{c}_K \right). \quad (4)$$

Here each entry $\partial r_n / \partial x_m$ in $\mathbf{A}$ is given by

$$\begin{cases} \frac{\partial r_n}{\partial x_m} \ne 0 & \text{if } x_m \text{ influences reaction } n, \\ \frac{\partial r_n}{\partial x_m} = 0 & \text{otherwise.} \end{cases} \quad (5)$$

See (13) for an example. Note that whether each entry in $\mathbf{A}$ is zero or nonzero is determined structurally (i.e. only from information of the stoichiometric matrix ν and the qualitative dependence (5)). Also note that, qualitatively, the responses $\delta_{\hat{n}} x_m$ and $\delta_{\hat{n}} r_n$ are given by entries of $-\mathbf{A}^{-1}$, since the right-hand side of (3) can be regarded as -1 times the identity matrix (when $\frac{\partial r_n}{\partial k_n} \delta k_n > 0$).

For a given network Γ, we consider a pair $\Gamma_s = (\mathfrak{m}, \mathfrak{n})$ of a chemical subset $\mathfrak{m}$ and a reaction subset $\mathfrak{n}$ such that $\mathfrak{n}$ includes all reactions influenced by chemicals in $\mathfrak{m}$ (in the sense of (5)). We call such a Γ_s as *output-complete*. For a subnetwork $\Gamma_s = (\mathfrak{m}, \mathfrak{n})$, we define the *index* $\chi(\Gamma_s)$ as

$$\chi(\Gamma_s) = |\mathfrak{m}| - |\mathfrak{n}| + (\#cycle). \quad (6)$$

Here, $|\mathfrak{m}|$ and $|\mathfrak{n}|$ are the numbers of elements of the sets $\mathfrak{m}$ and $\mathfrak{n}$, respectively. $\#cycle$ is the number of independent kernel vectors of ν whose supports are contained in $\mathfrak{n}$. In general, $\chi(\Gamma_s)$ is non-positive (see [6]). Then a *buffering structure* is defined as an output-complete subnetwork Γ_s with $\chi(\Gamma_s) = 0$.

Suppose $\Gamma_s = (\mathfrak{m}, \mathfrak{n})$ is a buffering structure. By permutating the column and row indices, the matrix $\mathbf{A}$ can be written as follows: [6]

$$\mathbf{A} = \ |\mathfrak{n}| \updownarrow \ \overbrace{\begin{pmatrix} \mathbf{A}_{\Gamma_s} \\ square & * \\ \hline \mathbf{0} & \mathbf{A}_{\bar{\Gamma}_s} \end{pmatrix}}^{|\mathfrak{m}|+(\#cycle)}, \quad (7)$$

where the rows (columns) of $\mathbf{A}_{\Gamma_s}$ are associated with the reactions (chemicals and cycles) in Γ_s. Similarly, those of $\mathbf{A}_{\bar{\Gamma}_s}$ are associated with the complement $\bar{\Gamma}_s := \Gamma \backslash \Gamma_s$.

The *law of localization* [6] is a consequence of the block structure (7) of $\mathbf{A}$: *Steady-state concentrations and fluxes outside of a buffering structure does not change under any rate parameter perturbations in $\mathfrak{n}$.* In other words, all effects of perturbations of $k_{\hat{n}}$ in $\mathfrak{n}$ are indeed localized within Γ_s.

III. STRUCTURAL BIFURCATION ANALYSIS

We shortly sketch the conventional bifurcation analysis (see for example [10–14]). Set $J := \nu \frac{\partial \boldsymbol{r}}{\partial \boldsymbol{x}}|_{\boldsymbol{x}=\boldsymbol{x}^*}$. Let the eigenvalues $\{\sigma_m\}_{m=1}^{M}$ of J be ordered so that $\operatorname{Re}\sigma_1 \ge \operatorname{Re}\sigma_2 \ge \ldots \ge \operatorname{Re}\sigma_n$. Then the state $\boldsymbol{x}^*$ is stable if all $\operatorname{Re}\sigma_m < 0$, whereas, the state $\boldsymbol{x}^*$ is unstable if $\operatorname{Re}\sigma_1 > 0$. Moreover, a bifurcation occurs if $\operatorname{Re}\sigma_1$ changes its sign as some parameter $k_{\hat{n}}$ is varied through some critical value, say $\bar{k}_{\hat{n}}$. Since $\det J = \prod_{m=1}^{M} \sigma_m$, a bifurcation occurs if $\det J$ changes its sign as $k_{\hat{n}}$ is varied through $\bar{k}_{\hat{n}}$. Thus,

the study of onset of bifurcation is reduced to search of zeros of det J.

The standard bifurcation analysis is based on the Jacobian matrix of (1). However, the network structures and the reaction rates are indistinguishably mixed in the Jacobian matrix J. Thus, it is difficult to perform bifurcation analysis of large systems based on the Jacobian. In the following, we present a method to perform bifurcation analysis directly from network structures, which is available even when networks are large.

Now, we explain *structural bifurcation analysis*. The key relation is (see Appendix A for the proof.)

$$\det J \propto \det \mathbf{A}, \tag{8}$$

Then (8) implies that the study of onset of bifurcation can be reduced to search of zeros of det $\mathbf{A}$. Further, the existence of the buffering structure Γ_s leads to

$$\det J \propto \det \mathbf{A}_{\Gamma_s} \cdot \det \mathbf{A}_{\bar{\Gamma}_s}. \tag{9}$$

With the use of additional facts which are stated below and proven in Appendix, we can derive several implications from the factorization (9). First, when det $J = 0$, we have either det $\mathbf{A}_{\Gamma_s} = 0$ or det $\mathbf{A}_{\bar{\Gamma}_s} = 0$. Therefore, the possibility of bifurcation occurrences in the whole system can be studied by examining the possibility for each determinant structure, based on network structures.

Second, from the law of localization, det $\mathbf{A}_{\bar{\Gamma}_s}$ depends only on parameters outside Γ_s. By contrast, det $\mathbf{A}_{\Gamma_s}$ depends on parameters in the whole network Γ (see Appendix B 2 for the rigorous proof). Thus, bifurcations associated with det $\mathbf{A}_{\bar{\Gamma}_s}$ are triggered only by tuning parameters in $\bar{\Gamma}_s$, while bifurcations associated with det $\mathbf{A}_{\Gamma_s}$ can be induced by both parameters in Γ_s and those in $\bar{\Gamma}_s$ (see inducing parameters in Fig. 1 (4)). In particular, in the former case, critical values (values at bifurcation points) of parameters in $\bar{\Gamma}_s$ are independent of parameters in Γ_s.

Third, the null vector of J at a bifurcation point with det $\mathbf{A}_{\Gamma_s} = 0$ has nonzero components only for chemicals in Γ_s, whose proof is postponed to Appendix C for simplicity. This implies that only chemicals in Γ_s exhibit bifurcations at this bifurcation point. By contrast, for bifurcations associated with det $\mathbf{A}_{\bar{\Gamma}_s}$, all chemicals in Γ exhibit bifurcations (see bifurcating chemicals in Fig. 1 (5)).

Equation (9) can be extended to multiple buffering structures. For example, a nested sequence of buffering structures $\Gamma_1 \subset \ldots \subset \Gamma_L$ gives the relation det $J \propto$ det $\mathbf{A}_{\Gamma_1} \prod_{s=1}^{L-1} \det \mathbf{A}_{\Gamma_{s+1} \setminus \Gamma_s}$ (see Appendix B 3 for nonnested cases). Together with the above three arguments for a single buffering structure, we can have the following three principles for multiple buffering structures:

(i) *Factorization*: The bifurcation behaviors in a complex network can be studied by decomposing it into smaller subnetworks called *determinant structures*, which are defined as buffering structures with subtraction of their inner buffering structures (Fig. 1 (3)). For each

determinant structure, the condition for bifurcation occurrence can be examined from its network structure.

(ii) *Inducing parameters*: For each determinant structure D, the bifurcation parameters associated with det $\mathbf{A}_D = 0$, termed as the inducing parameters for D, are identifiable on the network. The bifurcations are induced by the parameters which are outside any buffering structures non-intersecting with the determinant structure D (Fig. 1 (4)).

(iii) *Bifurcating chemicals (and fluxes)*: For each determinant structure D, the chemicals exhibiting bifurcation behaviors associated with det $\mathbf{A}_D = 0$, termed as the bifurcating chemicals for D, are identifiable on the network. When the bifurcation condition is satisfied, the bifurcation of steady-state concentrations (and fluxes) appears only inside the (minimal) buffering structure containing the determinant structure D (Fig. 1 (5)).
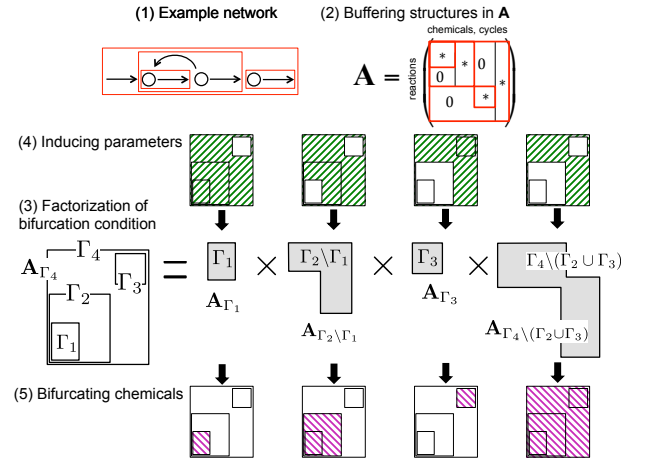
FIG. 1: Summary of the structural bifurcation analysis. (1) Buffering structures (red boxes) in an example network. (2) Buffering structures correspond to nonzero square blocks in $\mathbf{A}$. (3) Bifurcations are governed by the product of determinant structures: det $\mathbf{A} = $ det $\mathbf{A}_{\Gamma_1} \times$ det $\mathbf{A}_{\Gamma_2 \setminus \Gamma_1} \times$ det $\mathbf{A}_{\Gamma_3} \times$ det $\mathbf{A}_{\Gamma_4 \setminus (\Gamma_2 \cup \Gamma_3)}$. For each of the determinant structures, $\Gamma_1, \Gamma_2 \setminus \Gamma_1, \Gamma_3, \Gamma_4 \setminus (\Gamma_2 \cup \Gamma_3)$, the inducing parameters and bifurcating chemicals are shown by the shaded region in (4) and (5) respectively.

IV. HYPOTHETICAL NETWORK

We demonstrate the structural bifurcation analysis in the system in Fig. 2. The dynamics is described by the following differential equations:

$$\frac{d}{dt} \begin{pmatrix} x_A \\ x_B \\ x_C \end{pmatrix} = \nu \begin{pmatrix} r_1(k_1) \\ r_2(x_A; k_2) \\ r_3(x_A, x_B; k_3) \\ r_4(x_B, x_C; k_4) \\ r_5(x_B, x_C; k_5) \end{pmatrix} \tag{10}$$
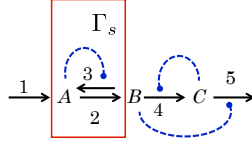
FIG. 2: System consisting of five reactions, $\xrightarrow{k_1} A$, $A \underset{k_2}{\overset{k_3}{\rightleftharpoons}} B$, $B \xrightarrow{k_4} C$, $C \xrightarrow{k_5}$. The three blue dashed arcs indicate the regulations explained in the text. The red box indicates a buffering structure Γ_s.

where the stoichiometric matrix ν is given by

$$\nu = \begin{pmatrix} 1 & -1 & 1 & 0 & 0 \\ 0 & 1 & -1 & -1 & 0 \\ 0 & 0 & 0 & 1 & -1 \end{pmatrix}. \qquad (11)$$

The kernel space of the matrix ν is spanned by

$$\boldsymbol{c}_1 = (0,1,1,0,0)^T, \boldsymbol{c}_2 = (1,1,0,1,1)^T. \qquad (12)$$

Every reaction rate depends on its substrate concentration. Reaction rates r_3, r_5, and r_4 are also regulated by A, B, and C, respectively. Then, this system has a single buffering structure, $\Gamma_s = (\{A\}, \{2,3\})$ with $\chi(\Gamma_s) = 1 - 2 + 1 = 0$, as shown in Fig. 2. Therefore, this system has two determinant structures, Γ_s and $\bar{\Gamma}_s := (\{B,C\}, \{1,4,5\})$.

According to our theory, qualitative sensitivity (responses of concentrations and fluxes to parameter perturbations) and bifurcation behaviors are determined by the matrix $\mathbf{A}$. By permutating the row index as $\{2,3,1,4,5\}$ and the column index as $\{A, \boldsymbol{c}_1, B, C, \boldsymbol{c}_2\}$, the matrix $\mathbf{A}$ and the determinant are given by

$$\mathbf{A} = \left(\begin{array}{c|c} \mathbf{A}_{\Gamma_s} & * \\ \hline \mathbf{0} & \mathbf{A}_{\bar{\Gamma}_s} \end{array} \right) = \begin{pmatrix} r_{2,A} & 1 & 0 & 0 & 1 \\ r_{3,A} & 1 & r_{3,B} & 0 & 0 \\ 0 & 0 & 0 & 0 & 1 \\ 0 & 0 & r_{4,B} & r_{4,C} & 1 \\ 0 & 0 & r_{5,B} & r_{5,C} & 1 \end{pmatrix}, \qquad (13)$$

where nonzero $\frac{\partial r_n}{\partial x_m}|_{\boldsymbol{x}=\boldsymbol{x}^*}$ is written by $r_{n,m}$ (m = A, B, C), and, especially, the three entries, $r_{3,A}, r_{5,B}, r_{4,C}$, correspond to the three regulations in Fig. 2. We assume that rates increase as substrate concentrations increase, i.e. $r_{n,m} > 0$, which is satisfied both in the mass-action and the Michaelis-Menten schemes.

As we explained below (5), the qualitative sensitivity is given by $-\mathbf{A}^{-1}$, although we do not study it in detail here. Below, we study bifurcation behaviors of steady states of the system. The onset of bifurcations can be studied from the determinant,

$$\det \mathbf{A} = \underbrace{(r_{2,A} - r_{3,A})}_{\det \mathbf{A}_{\Gamma_s}} \underbrace{(r_{5,B} r_{4,C} - r_{4,B} r_{5,C})}_{\det \mathbf{A}_{\bar{\Gamma}_s}}, \qquad (14)$$

where each factor corresponds to a determinant structure (Γ_s and $\bar{\Gamma}_s$, respectively). Since $r_{n,m} > 0$, the expression

of $\det \mathbf{A}$ implies that the regulation of r_3 by A (i.e. $r_{3,A}$) is necessary for the bifurcation associated with $\det \mathbf{A}_{\Gamma_s} = 0$. Similarly, both of the regulations of r_4 by C and r_5 by B (i.e. $r_{4,C}, r_{5,B}$) are necessary for the bifurcation associated with $\det \mathbf{A}_{\bar{\Gamma}_s} = 0$. In this way, the possibility of bifurcations and the regulatory conditions for it can be examined from structural information alone.

For numerical demonstration, we assume the following kinetics:

$$\boldsymbol{r} = \left(k_1, k_2 x_A, k_3 x_B \left(1 + \frac{k_{3,A} x_A^2}{x_A^2 + 5} \right), \right.$$
$$\left. k_4 x_B \left(1 + \frac{k_{4,C} x_C^2}{x_C^2 + 5} \right), k_5 x_C \left(1 + \frac{k_{5,B} x_B^2}{x_B^2 + 5} \right) \right)^T. \qquad (15)$$

The parameters are classified into $\{k_2, k_3, k_{3,A}\} \in \Gamma_s$, and $\{k_1, k_4, k_5, k_{4,C}, k_{5,B}\} \in \bar{\Gamma}_s$. We remark that the discussion in the remaining of this section is analytically predicted by our SBA theory in section III. The special choice of kinetics and the numerical computation are only for illustration of our theory.

First, we consider bifurcation associated with $\det \mathbf{A}_{\bar{\Gamma}_s}$. The inducing parameters for the determinant structure $\bar{\Gamma}_s$ are the parameters in $\bar{\Gamma}_s$ (the green-shaded region in Fig. 3 (A)). As seen from the plots of $\det \mathbf{A}_{\Gamma_s}$ and $\det \mathbf{A}_{\bar{\Gamma}_s}$ in Fig. 3 (a), the parameter $k_{5,B}$ in $\bar{\Gamma}_s$ actually induces sign changes of $\det \mathbf{A}_{\bar{\Gamma}_s}$ but not those of $\det \mathbf{A}_{\Gamma_s}$. The bifurcating chemicals for $\bar{\Gamma}_s$ are all chemicals $\{A, B, C\}$ (see the purple-shaded region in Fig. 3 (A)). Fig. 3 (a) actually shows that all of A, B, and C exhibit steady-state bifurcations.

Next, we consider the other bifurcation, which is associated with $\det \mathbf{A}_{\Gamma_s}$. The inducing parameters for the determinant structure Γ_s consist of all parameters in Γ_s and $\bar{\Gamma}_s$ (see the green-shaded region in the left panel of Fig. 3 (B)). The plots of $\det \mathbf{A}_{\Gamma_s}$ in Fig. 3 (b-1) show that the parameter $k_{3,A} \in \Gamma_s$ indeed induces bifurcations associated with $\det \mathbf{A}_{\Gamma_s}$. The bifurcating chemicals for Γ_s are the chemicals in Γ_s, i.e. $\{A\}$ (the purple-shaded region in Fig. 3 (B)). This can be confirmed from the plots for x_A^*, x_B^*, x_C^* in Fig. 3 (b-1), where only the steady-state of chemical $A \in \Gamma_s$ bifurcates at the bifurcation point, while chemicals B and $C \in \bar{\Gamma}_s$ remains constant as $k_{3,A} \in \Gamma_s$ is varied, due to the law of localization.

There is another choice of bifurcation parameter for the bifurcation associated with $\det \mathbf{A}_{\Gamma_s}$, as the inducing parameters for Γ_s are not only parameters in Γ_s but also those in $\bar{\Gamma}_s$ (see the green-shaded region in the left panel of Fig. 3 (B)). The parameter $k_{5,B} \in \bar{\Gamma}_s$, which was chosen as a bifurcation parameter in Fig. 3 (a), also induces the bifurcation associated with $\det \mathbf{A}_{\Gamma_s}$ (see the plots for $\det \mathbf{A}_{\Gamma_s}$ in Fig. 3 (b-2)). As in the case of Fig. 3 (b-1), the bifurcating chemicals are in Γ_s (see the purple-shaded region in Fig. 3 (B)). Thus we see that only chemical $A \in \Gamma_s$ bifurcates at the critical point in Fig. 3 (b-2).

In Fig. 3 (b-2), the non-bifurcating chemicals $\{B, C\}$ exhibit changes of their steady-state values to the change of the parameter $k_{5,B}$, while their values are constant in
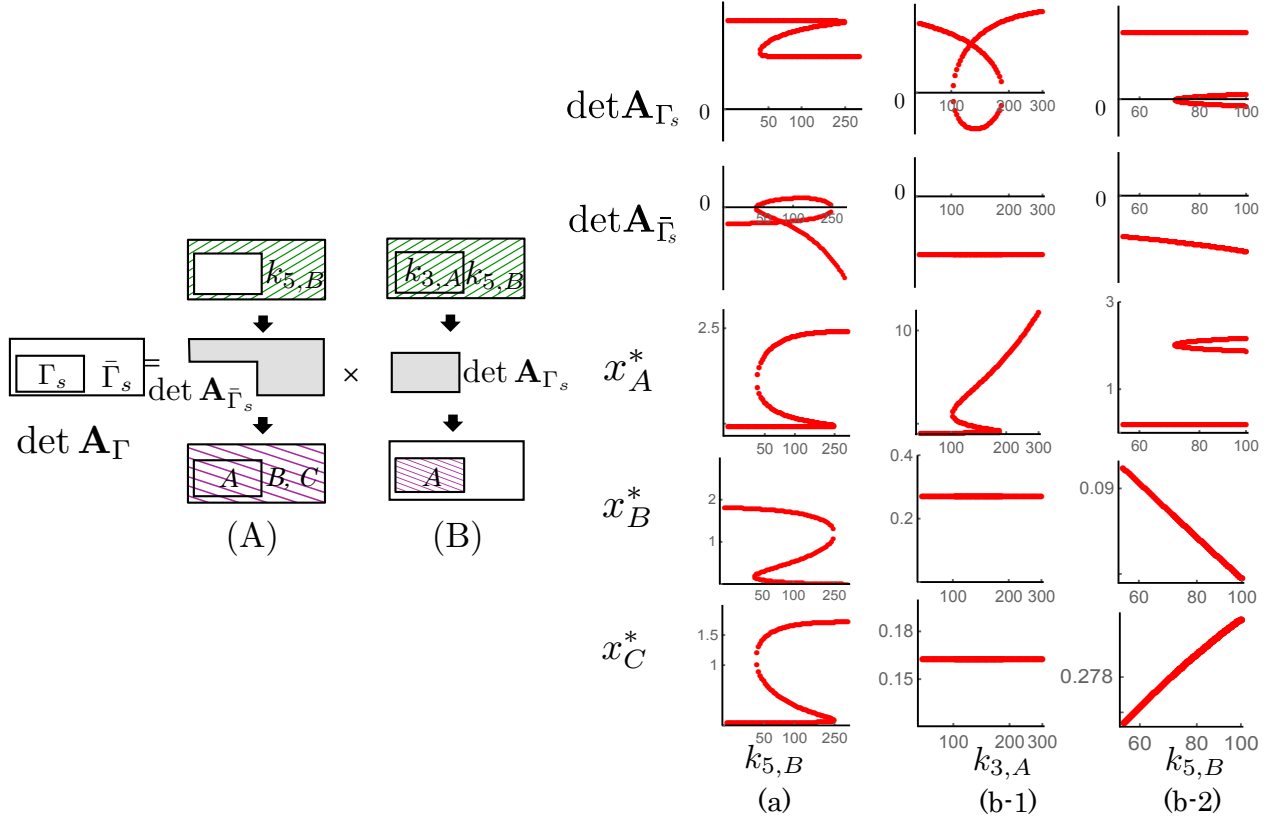
FIG. 3: Left panel: In (A) and (B), the dark-colored regions (at the middle) indicate determinant structures, and the green-shaded region (at the top) and purple-shaded region (at the bottom) indicate inducing parameters and bifurcating chemicals, respectively. Right panel: det $\mathbf{A}_{\Gamma_s}$, det $\mathbf{A}_{\bar{\Gamma}_s}$, x_A^*, x_B^*, x_C^* versus $k_{5,B}$ in (a), $k_{3,A}$ in (b-1), $k_{5,B}$ in (b-2). See Appendix E 4 for specific parameter values.

Fig. 3 (b-1). This difference in behaviors of the non-bifurcating chemicals can be understood by the law of localization: a parameter in $\bar{\Gamma}_s$ ($k_{5,B}$) influences all the chemicals in Γ_s and $\bar{\Gamma}_s$, while a parameter in Γ_s ($k_{3,A}$) influences only the chemical (A) in Γ_s.

Finally, we remark that although the same bifurcation parameter, $k_{5,B}$, is used in Fig. 3 (a) and Fig. 3 (b-2), different sets of chemicals exhibit bifurcation behaviors: While $k_{5,B}$ induces the bifurcations of all the chemicals in Fig. 3 (a), $k_{5,B}$ does not induce the bifurcations of chemicals in $\bar{\Gamma}_s$ in Fig. 3 (b-2). In this way, the same parameter may induce bifurcations for different sets of chemicals depending on which factor of det $\mathbf{A}_{\Gamma_s}$ and det $\mathbf{A}_{\bar{\Gamma}_s}$ changes its sign at the critical values of this parameter.

V. E. COLI NETWORK

The central carbon metabolic network is one of the most important networks in many organisms. The basic structures are shared between bacteria and human. In this network, glucose is decomposed into smaller metabolites and organisms obtain chemical energies through the reaction processes.

A cell may exhibit qualitatively different metabolic profiles, which are induced by, for example, enzyme modulations or environmental changes. A well-known example is the Warburg effect [15], where tumor cells utilize glycolysis to produce ATP even in the presence of oxygen. See also [8] for a study of environmental effects on bacteria. Theoretically, such qualitative change of metabolic states can be understood as bifurcation phenomena.

In this section, as an application of SBA to a real network, we study the central carbon metabolic network of E. coli [6] shown in Fig. 4, which consists of 28 metabolites and 46 reactions, including glycolysis, the tricarboxylic acid (TCA) cycle and the pentose phosphate pathway. We assume that each reaction rate function depends on its substrate concentrations.

The network possesses 17 determinant structures, as shown in Fig. 5, where each box represents a determinant structure. This in turn means that the matrix $\mathbf{A}$ has the structure shown in Fig. 6, where each square matrix corresponds to a buffering structure. In Fig. 6, the submatrix $\mathbf{A}_{\Gamma'}$ is associated with the determinant structure colored in green in Fig. 4 (corresponding to the glycolysis), and the submatrix $\mathbf{A}_{\Gamma''}$ is associated with the determinant structure colored in red in Fig. 4 (corresponding to the entrance of the TCA cycle from the glycolysis)
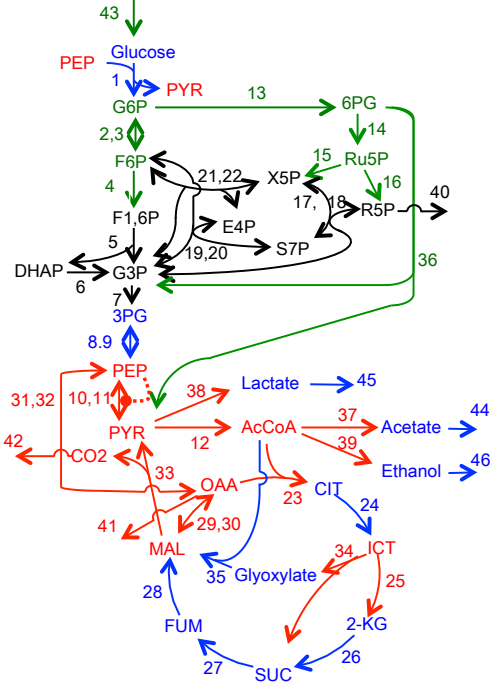
FIG. 4: Central carbon metabolic network of E. coli. Dashed curve indicates a regulation from PEP to reaction 11 ($r_{11,\text{PEP}} > 0$). Each pathway with a specific color (red, blue, green or black) is a determinant structure. In terms of buffering structures $\Gamma_s(s = 1, \ldots, 17)$ written in Appendix D, the blue subnetwork is $\Gamma_1 \cup \ldots \cup \Gamma_{10}$, and the black $\Gamma_{13} \cup \Gamma_{14} \cup \Gamma_{15} \cup \Gamma_{16}$. The red subnetwork Γ'' is given by Γ_{11} with subtraction of the blue subnetwork, and the green subnetwork Γ' is given by the whole network Γ_{17} with subtraction of the black subnetwork and Γ_{11}.
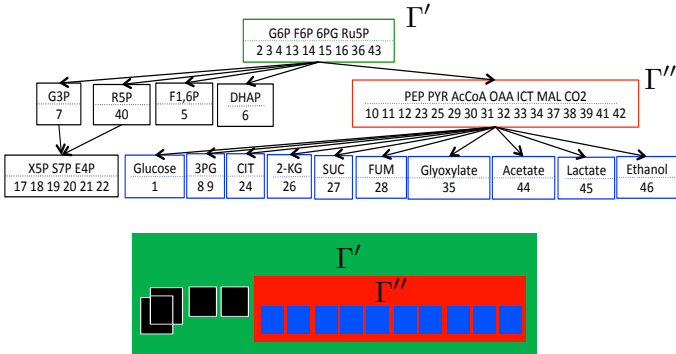
FIG. 5: Top panel: 17 determinant structures and their relationship. Each box, containing a set of chemicals and reactions (indicated by numbers), is a determinant structure. A box plus its downward boxes gives a buffering structure (see Appendix E 2 for the explicit list of buffering structures). Bottom panel: The schematic picture of the relationship corresponding to the top panel.

Thus, det $\mathbf{A}$ is factorized into 17 determinant factors.

FIG. 6: The matrix $\mathbf{A}$ of the E. coli network. There are 17 square submatrices (enclosed by lines) each of which corresponds to a buffering structure. See Appendix E 3 for the detailed expression of $\mathbf{A}$.

Up to a constant factor, it is given by

$$
\begin{aligned}
\det \mathbf{A} = {} & r_{1,\text{Glucose}} \times r_{5,\text{F1,6P}} \times r_{6,\text{DHAP}} \times r_{8,\text{3PG}} \\
& \times r_{44,\text{Acetate}} \times r_{45,\text{Lactate}} \times r_{46,\text{Ethanol}} \times r_{24,\text{CIT}} \\
& \times r_{26,\text{2-KG}} \times r_{27,\text{SUC}} \times r_{28,\text{FUM}} \times r_{35,\text{Glyoxylate}} \\
& \times r_{7,\text{G3P}} \times r_{40,\text{R5P}} \\
& \times \left(r_{17,\text{X5P}} r_{19,\text{S7P}} r_{21,\text{E4P}} + r_{18,\text{S7P}} r_{20,\text{E4P}} r_{21,\text{X5P}} \right) \\
& \times \det \mathbf{A}_{\Gamma'} \times \det \mathbf{A}_{\Gamma''}.
\end{aligned}
\tag{16}
$$

The explicit expressions for the factors $\det \mathbf{A}_{\Gamma'}, \det \mathbf{A}_{\Gamma''}$ are given in Appendix E (see (E4) and (E5)).

We can see from (16) that, among the 17 determinant structures, only the single determinant structure Γ'', colored in red in Fig. 4, has sign-changing determinant factors, and so can exhibit bifurcation. The reactions associated with the inducing parameters for the determinant structure Γ'' are colored in red and green (corresponding to the glycolysis and the entrance of the TCA cycle). The bifurcating chemicals (and fluxes) are colored in blue and red (corresponding to the TCA cycle and its entrance). Again these conclusions are independent of the choice of kinetics and rate parameters. For an illustration for these analytical findings, we use the mass-action kinetics with reaction 11 regulated by PEP in Fig. 7 (see Appendix E4 for details). Finally, the biological implications of these aforementioned results are given in the next section.

VI. CONCLUSIONS AND PERSPECTIVES

In this paper we proposed a mathematical method, SBA, to study bifurcation behaviors of reaction systems from network structures alone. In our method, bifurcations of the whole complex system are studied by factorizing it into smaller subnetworks (determinant structures), which are defined from local topology of the network. For each determinant structure, the bifurcation condition is studied, and a set of parameters possibly inducing the onset of bifurcations and a set of chemicals exhibiting bifurcation behaviors are determined. While biological functions are considered to arise from dynamics based
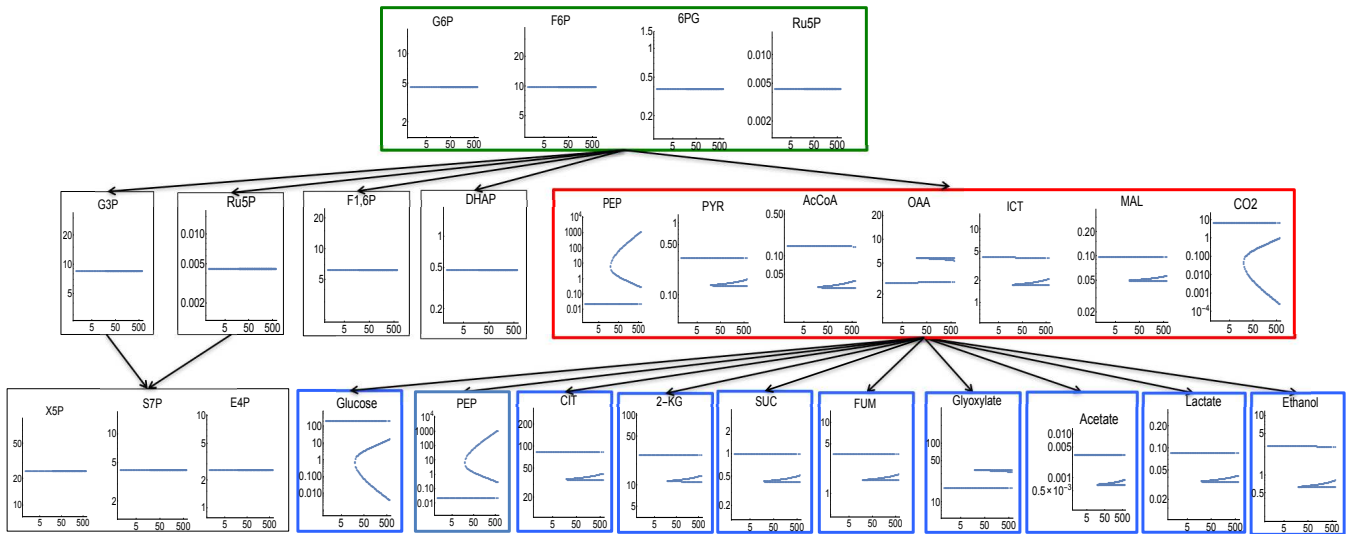
FIG. 7: Steady-state concentrations versus the parameter $k_{11,\mathrm{PEP}}$ in the E. coli system. Each box corresponds to the one in Fig. 5. A saddle-node bifurcation is observed only for the bifurcating chemicals for Γ'': Each chemical in the red and blue boxes (at the lower-right part) has one stable branch when $k_{11,\mathrm{PEP}}$ is small, and has two stable and one unstable branches when $k_{11,\mathrm{PEP}}$ is large. Each chemical in the green box (at the top) and black boxes (at the lower-left part) is independent of $k_{11,\mathrm{PEP}}$, due to the law of localization, and has one stable branch. See Appendix for the kinetics and the parameter values used here.

on reaction networks and modulation of enzymes, the complexity of networks has been a large obstacle to understand such systems. Our theory should be strongly effective to study behaviors of complex networks and promote systematic understandings of biological systems.

Our method is applicable to any steady-state bifurcations even if reaction systems have cokernel vectors. In the SM, we apply our theory to a phosphorylation system [16] with cokernel vectors (i.e. conserved concentrations), and the First Schlögl Model [17], exhibiting transcritical bifurcations.

One of the advantages of our method is that our method utilizes only information of the network structure and do not assume other quantitative details. Most of previous theoretical studies of chemical reaction systems assume specific kinetics and parameter values for reaction rate functions, more or less arbitrarily. In the framework of mass-action kinetics, a plenty of theoretically interesting results have been obtained (e.g. see [18–23]). However, it is not known whether these results could be applied to the system with different types of kinetics. Moreover, it would be difficult to determine actual kinetics of reactions in living cells precisely.

Another advantage of our method is that we can decompose a network into smaller subnetworks, through factorization of the bifurcation condition based on network topology. Our method is especially useful to study large networks such as metabolic networks. In the central carbon metabolism, we demonstrated that, if the network information is correct, bifurcations can be induced by enzymatic changes in the glycolysis and the entrance part of the TCA cycle, and bifurcation behaviors can be

observed only for the metabolites and fluxes inside.

We note that, under the assumption of the mass-action kinetics, Clarke [25–27] introduced stoichiometric network analysis to the study of complex reaction networks. His theory allows one to conclude that the reaction rates $(\mathbf{r}^*)$ associated with the positive steady states $(\mathbf{x}^*)$ is the convex linear combination of nonnegative kernel vectors of the stoichiometric matrix of the system, which are conventionally termed as extreme currents [27]. This correspondence was rigorously shown by Gatermann, Eiswirth, and Sensse [28] via the theory of algebraic geometry in the mass-action scheme. The mass-action assumption also allows one to rewrite the Jacobian of the sytem evaluated at any positive steady state as a convex combination of contributions from extreme currents. The bifurcation analysis can be performed by searching for all of possible convex combinations, which were carried out for some specific examples by Clarke and his coauthors [24, 29]. Although Clarke's theory can work well for the existence of positive steady states and give a method to perform bifurcation analysis of systems with mass-action kinetics, it cannot work for systems with non-mass-action kinetics. Also, even if network systems obey mass-action law, the Clarke's approach is not efficient for detecting bifurcation points if a network is large.

We can expect to use our theory as a tool to reveal unknown reactions or unknown regulations of chemical networks by combining theory with experimental measurements. Our knowledge of chemical reaction networks of many organisms is possibly incomplete, at present. We can compare our prediction of bifurcation behaviors

based on a "known" network with experimental observations. If our prediction disagrees with the experimental results, it will imply incompleteness of the network information.

Finally, our study might suggest an evolutionary origin of bifurcation behaviors. The theory implies that bifurcation behavior, qualitative change of behavior, emerges modularly in reaction systems, and that the modularity originates from network structures, i.e. determinant structures. It is suggestive, from evolutionary viewpoints, that, in the metabolic network, mathematically defined modules of plasticity (i.e. determinant structures) overlap with pathways identified from biological functions: the green in Fig. 4 corresponds to the glycolysis, the black to the pentose-phosphate pathway, the blue to the TCA cycle, and the red to the entrance of the TCA cycle.

Appendix A: The equivalence between the Jacobian matrix and the matrix A when $K_c = 0$

To establish (8) (or more precisely (A6)), we first note that the assumption $\dim \operatorname{coker} \nu := K_c = 0$ implies that $N \geq M$ and $K = N - M$, where $K := \dim \ker \nu$. Note that, in general, for any $M \times N$ matrix ν, the identity $M + \dim \ker \nu = N + \dim \operatorname{coker} \nu$ holds. Then employing the QR decomposition to the matrix ν^T, we can factor the ν^T as the product of an $N \times N$ unitary matrix $\mathbf{Q}$ and an $N \times M$ upper triangular matrix $\tilde{\mathbf{S}}^T$ where $\tilde{\mathbf{S}}^T$ is the transpose of the matrix $\tilde{\mathbf{S}}$. As the bottom K rows of an $N \times M$ upper triangular matrix consist entirely of zeroes, we thus have

$$\nu^T = \mathbf{Q}\tilde{\mathbf{S}}^T = [\mathbf{Q}_1 \ \mathbf{Q}_2] \begin{bmatrix} \mathbf{S}^T \\ \mathbf{0}_{K \times M} \end{bmatrix} = \mathbf{Q}_1 \mathbf{S}^T, \quad (A1)$$

where $\mathbf{S}^T$ is an $M \times M$ upper triangular matrix, $\mathbf{0}_{K \times M}$ is the $K \times M$ zero matrix, $\mathbf{Q}_1$ is a $N \times M$ matrix, $\mathbf{Q}_2$ is a $N \times K$ matrix, and both $\mathbf{Q}_1$ and $\mathbf{Q}_2$ have orthogonal columns. Further, the column space of $\mathbf{Q}_1$ is equal to the row space of ν, whereas the column space of $\mathbf{Q}_2$ is equal to the null space of ν, which follows from the fact that the row space of any nontrivial matrix is the orthogonal complement to its null space. To summarize, we have $\nu =$

$\mathbf{SQ}_1^T$. For simplicity, we let the basis $\{-\mathbf{c}_\alpha\}_{\alpha=1}^K$ consist of the columns of $\mathbf{Q}_2$.

Set $\mathbf{w} = [\mathbf{w}_1 \ \mathbf{w}_2]^T := \mathbf{Q}^T \frac{\partial \mathbf{r}}{\partial \mathbf{x}}$, where $\mathbf{w}_1$ is a $M \times M$ matrix, and $\mathbf{w}_2$ is a $K \times M$ matrix. Recall that $\mathbf{QQ}^T = I_N$. Then we can rewrite the matrix $\frac{\partial \mathbf{r}}{\partial \mathbf{x}}$ of $\mathbf{r}$ at the steady state $\mathbf{x}^*$ as follows:

$$\frac{\partial \mathbf{r}}{\partial \mathbf{x}} = \mathbf{Q}(\mathbf{Q}^T \frac{\partial \mathbf{r}}{\partial \mathbf{x}}) = [\mathbf{Q}_1 \ \mathbf{Q}_2] \begin{bmatrix} \mathbf{w}_1 \\ \mathbf{w}_2 \end{bmatrix} = \mathbf{Q}_1 \mathbf{w}_1 + \mathbf{Q}_2 \mathbf{w}_2. \tag{A2}$$

Together with (A1) and the orthogonal property of $\mathbf{Q}$, we can deduce that

$$J = \nu \frac{\partial \mathbf{r}}{\partial \mathbf{x}} = (\mathbf{SQ}_1^T)(\mathbf{Q}_1 \mathbf{w}_1 + \mathbf{Q}_2 \mathbf{w}_2) = \mathbf{Sw}_1. \tag{A3}$$

This in turn implies $\det(J) = \det(\mathbf{S}) \det(\mathbf{w}_1)$. Recall that the rank ($\operatorname{rank}(\nu)$) of the matrix ν is M. Then we have $\operatorname{rank}(\mathbf{S}) = \operatorname{rank}(\mathbf{SQ}_1^T) = \operatorname{rank}(\nu) = M$. Hence $\mathbf{S}$ is a square matrix of full rank, and so we can conclude that

$$\det(\mathbf{w}_1) = (\det(\mathbf{S}))^{-1} \det(J). \tag{A4}$$

On the other hand, in view of the orthogonal properties of $\mathbf{Q}, \mathbf{Q}_1$, and $\mathbf{Q}_2$, the matrix $\mathbf{A}$ (defined in the main text) can be written as

$$\mathbf{A} = [\frac{\partial \mathbf{r}}{\partial \mathbf{x}} \ \mathbf{Q}_2] = [\mathbf{Qw} \ \mathbf{Q}_2] = \mathbf{Q}[\mathbf{w} \ \mathbf{Q}^T \mathbf{Q}_2] = \mathbf{Q} \begin{bmatrix} \mathbf{w}_1 & \mathbf{0}_{M \times K} \\ \mathbf{w}_2 & I_K \end{bmatrix}.$$

Since $\mathbf{Q}$ is a square orthogonal matrix with $\det(\mathbf{Q}) = \pm 1$, we can thus deduce

$$\det(\mathbf{w}_1) = \pm \det(\mathbf{A}). \tag{A5}$$

Then from (A4) and (A5), we obtain the following result.

Theorem 1

$$\det(\mathbf{A}) = \pm \frac{\det(J)}{\det(\mathbf{S})}. \tag{A6}$$

Appendix B: Structural Factorization of det A when $K_c = 0$

Here, we explain the factorization of $\mathbf{A}$ after reviewing buffering structures and the law of localization when $K_c = 0$.

1. Buffering structure and the law of localization when $K_c = 0$ (review of [6])

We construct a *subnetwork* $\Gamma_s = (\mathfrak{m}, \mathfrak{n})$, a pair of chemicals and reactions, as follows:

1. Choose a subset $\mathfrak{m} \subseteq \mathbb{X}$ of chemicals.

2. Choose a subset $\mathfrak{n} \subseteq \mathbb{E}$ of reactions such that $\mathfrak{n}$ includes any reaction n whose rate function $r_n(\mathbf{x})$ is regulated by (at least one member in) $\mathfrak{m}$ (namely, $\frac{\partial r_n}{\partial x_m} \neq 0$ for some $m \in \mathfrak{m}$). In other words, we can construct $\mathfrak{n}$ by collecting all reactions n that are regulated by $\mathfrak{m}$ plus any other reactions.

We call a subnetwork satisfying the above conditions *output-complete*. Below, we consider only output-complete subnetworks. To proceed, we introduce the definition that a kernel vector $\mathbf{v} \in \mathbb{R}^N$ has support contained in $\mathfrak{n}$. Indeed, for the reaction subset $\mathfrak{n}$, we can associate the vector space $V(\mathfrak{n})$:

$$V(\mathfrak{n}) := \mathrm{span}\left\{\mathbf{v}\,|\,\mathbf{v} \in \ker \nu,\, P^{\mathfrak{n}}\mathbf{v} = \mathbf{v}\right\}.$$

Here, $P^{\mathfrak{n}}$ is an $N \times N$ projection matrix onto the space associated with $\mathfrak{n}$ defined by

$$P^{\mathfrak{n}}_{n,n'} = \delta_{n,n'} \text{ if } n, n' \in \mathfrak{n}. \text{ Otherwise } P^{\mathfrak{n}}_{n,n'} = 0.$$

Then we say that a kernel vector $\mathbf{v} \in \mathbb{R}^N$ has support contained in $\mathfrak{n}$ if $\mathbf{v} \in V(\mathfrak{n})$.

For a subnetwork $\Gamma_s = (\mathfrak{m}, \mathfrak{n})$, we define the *index* $\chi(\Gamma_s)$ by the relation

$$\chi(\Gamma_s) = |\mathfrak{m}| - |\mathfrak{n}| + (\#cycle). \tag{B1}$$

Here, $|\mathfrak{m}|$ and $|\mathfrak{n}|$ are the number of elements in the sets $\mathfrak{m}$ and $\mathfrak{n}$, respectively. The $\#cycle$ is the number of independent kernel vectors of the matrix ν whose supports are contained in $\mathfrak{n}$. In general, $\chi(\Gamma_s)$ is non-positive (see [6]).

Then a *buffering structure* is defined as a subnetwork Γ_s with $\chi(\Gamma_s) = 0$.

It was proved in [6] that, for a buffering structure $\Gamma_s = (\mathfrak{m}, \mathfrak{n})$, the steady state values of chemical concentrations and reaction rates outside Γ_s are independent of the reaction rate parameters k_n of reactions in $\mathfrak{n}$. Specifically, let $\boldsymbol{x}^* = (x_1^*, \ldots, x_M^*)$ be the steady state of (1). Note that $\boldsymbol{x}^*$ depends on the parameter vector $\boldsymbol{k} = (k_1, \ldots, k_N)^T$. Set

$$\boldsymbol{r}^* = (r_1^*, \ldots, r_N^*) := (r_1(\boldsymbol{x}^*; k_1), \ldots, r_N(\boldsymbol{x}^*; k_N)).$$

Then, for any $n' \in \mathfrak{n}$, and any $m \in \mathfrak{m}^c$ and $n \in \mathfrak{n}^c$, one has

$$\frac{\partial x_m^*}{\partial k_{n'}} = 0, \quad \frac{\partial r_n^*}{\partial k_{n'}} = 0, \tag{B2}$$

where $\mathfrak{m}^c = \mathbb{X} \setminus \mathfrak{m}$ and $\mathfrak{n}^c = \mathbb{E} \setminus \mathfrak{n}$ are the complementary set of $\mathfrak{m}$ and $\mathfrak{n}$, respectively. For ease of notation, we set

$$\bar{\Gamma}_s := (\mathfrak{m}^c, \mathfrak{n}^c).$$

We remark that a whole network Γ always satisfies the condition of the law of localization because $\chi(\Gamma) = M - N + K = K_c = 0$.

2. Factorization of the matrix A for a single buffering structure when $K_c = 0$

Suppose that Γ_s is a buffering structure. Then, by permuting the columns and rows of the matrix $\mathbf{A}$, the resulting matrix (still denoted by $\mathbf{A}$ for simplicity) can be written in the following form [6]:

$$\mathbf{A} = \begin{pmatrix} \mathbf{A}_{\Gamma_s} & \mathbf{A}_{\Gamma_s, \bar{\Gamma}_s} \\ \mathbf{0}_{|\mathfrak{n}^c| \times |\mathfrak{n}|} & \mathbf{A}_{\bar{\Gamma}_s} \end{pmatrix}. \tag{B3}$$

In the following, for ease of presentation, for a subnetwork $\Gamma_s = (\mathfrak{m}, \mathfrak{n})$, if no confusions can arise, we write $(m, n) \in \Gamma_s$ instead of "$m \in \mathfrak{m}$ and $n \in \mathfrak{n}$". The entries of $\mathbf{A}_{\Gamma_s}$ consist of components of the constant vectors $\mathbf{v} \in V(\mathfrak{n})$, and the term $\frac{\partial r_n}{\partial x_m}\big|_{\boldsymbol{x}=\boldsymbol{x}^*}$ with $(m, n) \in \Gamma_s$, which corresponds to self-regulations inside Γ_s (regulations from chemicals in Γ_s to reaction rate functions in Γ_s). Similar characteristics for the entries of $\mathbf{A}_{\bar{\Gamma}_s}$ can be observed, which corresponds to self-regulations inside the complementary part $\bar{\Gamma}_s$. The non-constant entries of the upper-right matrix $\mathbf{A}_{\Gamma_s, \bar{\Gamma}_s}$ correspond to regulations from $\bar{\Gamma}_s$ to Γ_s. Finally, the lower-left block in (B3) is the zero matrix because (i) the kernel vectors in Γ_s do not have support on reactions in $\mathfrak{n}^c$ and (ii) $\partial r_n / \partial x_m = 0$ for $n \in \mathfrak{n}^c$, $m \in \mathfrak{m}$, which follows from the condition that Γ_s is output-complete (see also [6]).

We have the following results.

Theorem 2 *The followings hold for a reaction network Γ with a buffering structure Γ_s.*

(i) *The determinant of the matrix $\mathbf{A}$ can be factorized as follows:*

$$\det \mathbf{A} = \det \mathbf{A}_{\Gamma_s} \times \det \mathbf{A}_{\bar{\Gamma}_s}. \tag{B4}$$

Note that $\mathbf{A}_{\Gamma_s, \bar{\Gamma}_s}$ does not contribute to $\det \mathbf{A}$.

(ii)

$$\frac{\partial \mathbf{A}_{\bar{\Gamma}_s}}{\partial k_n} = 0 \quad \text{for } n \in \mathfrak{n}. \tag{B5}$$

Thus the complementary part $\mathbf{A}_{\bar{\Gamma}_s}$ is independent of the rate parameters k_n with $n \in \mathfrak{n}$.

The assertion (i) follows from the block structure shown in (B3). The assertion (ii) can be proved as follows: The entries of $\mathbf{A}_{\bar{\Gamma}_s}$ consist of the term $\frac{\partial r_{n'}}{\partial x_{m'}}\big|_{\boldsymbol{x}=\boldsymbol{x}^*}$ with $(m', n') \in (\mathfrak{m}^c, \mathfrak{n}^c)$ and the components of the kernel vectors of the matrix ν, which is obviously independent of k_n for each $n = 1, \ldots, N$. From the construction of the subnetwork Γ_s, $r_{n'}$ are functions of variables $x_{m'}$ with $m' \in \mathfrak{m}^c$ (because, if the function $r_{n'}$ depended also on x_m with $m \in \mathfrak{m}$, such a reaction n' should be included into Γ_s, by construction of the subnetwork Γ_s). Therefore, the derivatives $\frac{\partial r_{n'}}{\partial x_{m'}}\big|_{\boldsymbol{x}=\boldsymbol{x}^*}$ can be written in terms of $x_{m'}^*$ with $m' \in \mathfrak{m}^c$. Then, these derivatives $\frac{\partial r_{n'}}{\partial x_{m'}}\big|_{\boldsymbol{x}=\boldsymbol{x}^*}$ are independent of k_n for $n \in \mathfrak{n}$ due to (B2).

An important remark is that the above theorem can be applied not only to a single buffering structure but also for nested buffering structures. For example, a buffering structure within another larger buffering structure is

studied similarly, by regarding Γ as a larger buffering structure and Γ_s as a smaller buffering structure in it. Note that, as we remarked before, a whole network Γ is always a buffering structure.

In summary, for a buffering structure Γ_s inside a network Γ, we have proved

$$\det \mathbf{A}_\Gamma = \det (\mathbf{A}_{\Gamma_s} \times \underbrace{\det \mathbf{A}_{\bar{\Gamma}_s}}_{\substack{\text{independent of} \\ k_{\Gamma_s}}} , \qquad \text{(B6)}$$

where k_{Γ_s} denotes the set of parameters of reactions inside Γ_s.

3. Factorization of the matrix A for multiple buffering structures when $K_c = 0$

We generalize the above factorization formula (B6) into multiple buffering structures.

First, we consider a network Γ containing L non-intersecting buffering structures $\Gamma_1, \ldots, \Gamma_L$. We write the complement of the buffering structures as $\bar{\Gamma}_{1,\ldots,L} := \Gamma \backslash (\Gamma_1 \cup \ldots \cup \Gamma_L)$, and so Γ can be decomposed as

$$\Gamma = \Gamma_1 \cup \ldots \cup \Gamma_L \cup \bar{\Gamma}_{1,\ldots,L}. \qquad \text{(B7)}$$

For each buffering structure Γ_s, the columns associated with chemicals and cycles in Γ_s have nonzero entries only for reactions in Γ_s, by the same reason explained below (B3). Thus, the matrix $\mathbf{A}$ can be written in the following form:

$$\mathbf{A} = \begin{pmatrix} \boxed{\mathbf{A}_{\Gamma_1}} & \mathbf{0} & \cdots & \mathbf{0} & \mathbf{A}_{\Gamma_1, \bar{\Gamma}_{1,\ldots,L}} \\ \mathbf{0} & \boxed{\mathbf{A}_{\Gamma_2}} & \cdots & \mathbf{0} & \mathbf{A}_{\Gamma_2, \bar{\Gamma}_{1,\ldots,L}} \\ \vdots & \vdots & \ddots & \vdots & \vdots \\ \mathbf{0} & \mathbf{0} & \cdots & \boxed{\mathbf{A}_{\Gamma_L}} & \mathbf{A}_{\Gamma_L, \bar{\Gamma}_{1,\ldots,L}} \\ \mathbf{0} & \mathbf{0} & \cdots & \mathbf{0} & \mathbf{A}_{\bar{\Gamma}_{1,\ldots,L}} \end{pmatrix}, \qquad \text{(B8)}$$

where each square matrix $\mathbf{A}_{\Gamma_s}$ ($s = 1, \ldots, L$) enclosed by lines is associated with the buffering structure Γ_s and defined as

$$\mathbf{A}_{\Gamma_s} = \left(\left(\frac{\partial \boldsymbol{r}}{\partial \boldsymbol{x}} \right)_{\Gamma_s} \middle| \boldsymbol{c}^s{}_1 \ \ldots \ \boldsymbol{c}^s{}_{K_s} \right). \qquad \text{(B9)}$$

Here, the left block, $(\frac{\partial \boldsymbol{r}}{\partial \boldsymbol{x}})_{\Gamma_s}$, consists of $\frac{\partial r_n}{\partial x_m}$ with $(m, n) \in \Gamma_s$, and the right block corresponds to the independent kernel vectors of ν whose support are on reactions in Γ_s (K_s is the number of the kernel vectors).

Then, we can prove that

$$\det \mathbf{A} = \left(\prod_{s=1}^{L} \underbrace{\det \mathbf{A}_{\Gamma_s}}_{\substack{\text{dependent on} \\ k_{\Gamma_s} \text{ and } k_{\bar{\Gamma}_{1,\ldots,L}}}} \right) \times \underbrace{\det \mathbf{A}_{\bar{\Gamma}_{1,\ldots,L}}}_{\substack{\text{dependent on} \\ k_{\bar{\Gamma}_{1,\ldots,L}}}}, \qquad \text{(B10)}$$

where $k_{\Gamma'}$ denotes the set of parameters associated with reactions inside a subnetwork Γ'. The parameter dependence is determined by using (B6) for every buffering
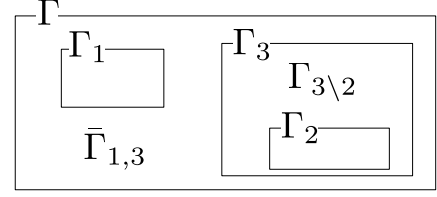

FIG. 8: Example network Γ. Rectangular boxes, Γ_1, Γ_2, Γ_3, indicate buffering structures. The law of localization indicates that k_{Γ_1} influences (steady-state values of chemicals and fluxes in) Γ_1, k_{Γ_3} influences Γ_3, $k_{\Gamma_{3\backslash 2}}$ influences Γ_2, and $k_{\bar{\Gamma}_{1,3}}$ influences the whole network Γ.

structure Γ_s ($s = 1, \ldots, L$). For example, (B6) for the buffering structure Γ_1 implies that the determinant factors except for $\det \mathbf{A}_{\Gamma_1}$ is independent of k_{Γ_1} and so on.

We can also factorize a nested sequence of buffering structures. Consider a network Γ consisting of a nested sequence of L buffering structures $\Gamma_1 \subset \ldots \subset \Gamma_L := \Gamma$. In this case, the matrix $\mathbf{A}$ can be written as

$$\mathbf{A} = \begin{pmatrix} \mathbf{A}_{\Gamma_1} & * & * & \cdots & * \\ \mathbf{0} & \mathbf{A}_{\Gamma_2 \backslash \Gamma_1} & & \cdots & * \\ \mathbf{0} & \mathbf{0} & \mathbf{A}_{\Gamma_3 \backslash \Gamma_2} & & \vdots \\ \vdots & \vdots & & \ddots & * \\ \mathbf{0} & \mathbf{0} & \cdots & \mathbf{0} & \mathbf{A}_{\Gamma_L \backslash \Gamma_{L-1}} \end{pmatrix}, \qquad \text{(B11)}$$

where $*$'s indicate nonzero blocks, and the nested block structure (indicated by lines) corresponds to the nested sequence of the buffering structures, $\Gamma_1, \ldots, \Gamma_L$. By using (B6) iteratively, we can prove

$$\det \mathbf{A} = \underbrace{\det \mathbf{A}_{\Gamma_1}}_{\substack{\text{dependent on} \\ k_{\Gamma_L}}} \prod_{s=1}^{L-1} \underbrace{\det \mathbf{A}_{\Gamma_{s+1} \backslash \Gamma_s}}_{\substack{\text{dependent on} \\ k_{\Gamma_{s+1} \backslash \Gamma_s}}}. \qquad \text{(B12)}$$

By using (B10) and (B12), we can factorize the determinant of $\mathbf{A}$ for multiple buffering structures and determine the parameter dependence for each factor. We illustrate the procedure of factorization in an example network (see Fig. 8): Suppose that a whole network Γ contains two non-intersecting buffering structures Γ_1 and Γ_3, and Γ_3 further contains a smaller buffering structure Γ_2 inside it;

$$\Gamma = \Gamma_1 \cup \Gamma_3 \cup \bar{\Gamma}_{1,3}$$
$$= \Gamma_1 \cup (\Gamma_2 \cup \Gamma_{3\backslash 2}) \cup \bar{\Gamma}_{1,3}. \qquad \text{(B13)}$$

Here, $\bar{\Gamma}_{1,3} := \Gamma \backslash (\Gamma_1 \cup \Gamma_3)$ and $\Gamma_{3\backslash 2} := \Gamma_3 \backslash \Gamma_2$. In this case, the matrix $\mathbf{A}$ can be written as

$$\mathbf{A} = \begin{pmatrix} \boxed{\mathbf{A}_{\Gamma_1}} & \mathbf{0} & * \\ \mathbf{0} & \boxed{\mathbf{A}_{\Gamma_3}} & * \\ \mathbf{0} & \mathbf{0} & \mathbf{A}_{\bar{\Gamma}_{1,3}} \end{pmatrix} = \begin{pmatrix} \boxed{\mathbf{A}_{\Gamma_1}} & \mathbf{0} & \mathbf{0} & * \\ \mathbf{0} & \boxed{\mathbf{A}_{\Gamma_2}} & * & * \\ \mathbf{0} & \mathbf{0} & \mathbf{A}_{\Gamma_{3\backslash 2}} & * \\ \mathbf{0} & \mathbf{0} & \mathbf{0} & \mathbf{A}_{\bar{\Gamma}_{1,3}} \end{pmatrix},$$

$$\text{(B14)}$$

where each square matrix enclosed by lines corresponds to a buffering structure. The determinant of $\mathbf{A}$ is factorized as

$$\det \mathbf{A} = \underbrace{\det \mathbf{A}_{\Gamma_1}}_{\substack{\text{depends on} \\ k_{\Gamma_1} \text{ and } k_{\bar{\Gamma}_{1,3}}}} \times \underbrace{\det \mathbf{A}_{\Gamma_3}}_{\substack{\text{depends on} \\ k_{\Gamma_3} \text{ and } k_{\bar{\Gamma}_{1,3}}}} \times \underbrace{\det \mathbf{A}_{\bar{\Gamma}_{1,3}}}_{\substack{\text{depends on} \\ k_{\bar{\Gamma}_{1,3}}}}$$

$$= \underbrace{\det \mathbf{A}_{\Gamma_1}}_{\substack{\text{depends on} \\ k_{\Gamma_1} \text{ and } k_{\bar{\Gamma}_{1,3}}}} \times (\underbrace{\det \mathbf{A}_{\Gamma_2}}_{\substack{\text{depends on} \\ k_{\Gamma_2}, k_{\Gamma_{3\backslash 2}}, \text{ and } k_{\bar{\Gamma}_{1,3}}}} \times \underbrace{\det \mathbf{A}_{\Gamma_{3\backslash 2}}}_{\substack{\text{depends on} \\ k_{\Gamma_{3\backslash 2}} \text{ and } k_{\bar{\Gamma}_{1,3}}}})$$

$$\times \underbrace{\det \mathbf{A}_{\bar{\Gamma}_{1,3}}}_{\substack{\text{depends on} \\ k_{\bar{\Gamma}_{1,3}}}} . \tag{B15}$$

In the first line, we have used (B10) with $L = 2$ for the whole network Γ. In the second line, we have used (B12) with $L = 2$, namely (B6), for the buffering structure Γ_3, where the factor $\det \mathbf{A}_{\Gamma_3}$ is factorized further and its dependence on k_{Γ_3} is determined more finely.

Appendix C: Equivalence between null vectors of A and J, and bifurcating chemicals when $K_c = 0$

Suppose that a chemical reaction system Γ with a buffering structure Γ_s exhibits steady-state bifurcations. At a bifurcation point, there exist null vectors for the matrix A and the Jacobian matrix J, since $\det \mathbf{A} = \det J = 0$. Note that, here, for J and $\mathbf{A}$, we call their eigenvectors with eigenvalue 0 null vectors, rather than kernel vectors, in order to distinguish them from kernel vectors of ν. In the presence of a buffering structure Γ_s, the bifurcation is associated with either $\det \mathbf{A}_{\Gamma_s} = 0$ or $\det \mathbf{A}_{\bar{\Gamma}_s} = 0$.

In this section, we show that, for a bifurcation associated with $\det \mathbf{A}_{\Gamma_s} = 0$, the corresponding null vector $\boldsymbol{v}$ of the Jacobian matrix J satisfies

$$v_m = 0 \quad \text{for chemical } m \in \bar{\Gamma}_s. \tag{C1}$$

Namely, the null vector $\boldsymbol{v}$ of J has support inside chemicals in Γ_s when $\det \mathbf{A}_{\Gamma_s} = 0$. This implies that, for a bifurcation associated with $\det \mathbf{A}_{\Gamma_s} = 0$, only chemicals inside Γ_s undergo a bifurcating behavior.

The strategy for showing (C1) is to use the null vectors of $\mathbf{A}_{\Gamma_s}$ to construct the associated null vector $\boldsymbol{v}$ of the Jacobian matrix J.

We consider a chemical reaction system of M chemicals and N reactions where the cokernel space of ν consists only of the zero vector. Suppose that $\det \mathbf{A}_{\Gamma_s} = 0$ whose associated buffering structure $\Gamma_s = (\mathfrak{m}, \mathfrak{n})$ contains $|\mathfrak{m}|$ chemicals, $|\mathfrak{n}|$ reactions, and $K_s = |\mathfrak{n}| - |\mathfrak{m}|$ kernel vectors, $\{\boldsymbol{c}^1, \ldots, \boldsymbol{c}^{K_s}\}$, of ν. By construction, each $\boldsymbol{c}^\alpha \in \mathbb{R}^N$ ($\alpha = 1, \ldots, K_s$) has support on reactions inside Γ_s, and thus has the following form,

$$\boldsymbol{c}^\alpha = \begin{pmatrix} \boldsymbol{c}'^\alpha \\ \hline \mathbf{0} \end{pmatrix}, \tag{C2}$$

where the upper $|\mathfrak{n}|$ components (resp. lower $N - |\mathfrak{n}|$ components) are associated with reactions in Γ_s (resp. $\bar{\Gamma}_s$). By using $\boldsymbol{c}'^\alpha$, $\mathbf{A}_{\Gamma_s}$ in (B3) can be written as

$$\mathbf{A}_{\Gamma_s} = \left((\frac{\partial \boldsymbol{r}}{\partial \boldsymbol{x}})_{\Gamma_s} \middle| -\boldsymbol{c}'^1 \ldots -\boldsymbol{c}'^{K_s} \right), \tag{C3}$$

where $(\frac{\partial \boldsymbol{r}}{\partial \boldsymbol{x}})_{\Gamma_s}$ is an $|\mathfrak{n}| \times |\mathfrak{m}|$ matrix whose (n, m) component is given by $\frac{\partial r_n}{\partial x_m}$ with $n \in \mathfrak{n}$ and $m \in \mathfrak{m}$.

Since $\det \mathbf{A}_{\Gamma_s} = 0$, there exist a null vector $\boldsymbol{u}_s \in \mathbb{R}^{|\mathfrak{m}| + K_s}$ such that

$$\mathbf{A}_{\Gamma_s} \boldsymbol{u}_s = 0. \tag{C4}$$

If we write $\boldsymbol{u}_s = (\eta_1, \ldots, \eta_{|\mathfrak{m}|}, \zeta_1, \ldots, \zeta_{K_s})$ and substitute $\mathbf{A}_{\Gamma_s}$ in (C3) into Eq. (C4), we obtain

$$\sum_{m \in \mathfrak{m}} \frac{\partial r_n}{\partial x_m} \eta_m - \sum_{\alpha=1}^{K_s} (\boldsymbol{c}'^\alpha)_n \zeta_\alpha = 0 \tag{C5}$$

for any reaction $n \in \mathfrak{n}$. Note that all indices in (C5) are associated with Γ_s.

In order to relate (C5) with the Jacobian matrix J of the whole system Γ, we rewrite (C5) using indices of the whole system. First, by using (C2) and $\frac{\partial r_n}{\partial x_m} = 0$ for $m \in \mathfrak{m}, n \in \mathfrak{n}^c$, corresponding to the fact that chemical concentrations in a buffering structure does not appear in the arguments of rate functions of reactions outside the buffering structure, we can rewrite (C5) as

$$\sum_{m \in \mathfrak{m}} \frac{\partial r_n}{\partial x_m} \eta_m - \sum_{\alpha=1}^{K_s} (\boldsymbol{c}^\alpha)_n \zeta_\alpha = 0, \tag{C6}$$

where n is any reaction in the whole system $\Gamma = (\mathbb{X}, \mathbb{E})$. Note that $\boldsymbol{c}'$ has been replaced by $\boldsymbol{c}$. Furthermore, by introducing an M-dimensional vector $\boldsymbol{v}$ as $\boldsymbol{v} = (\boldsymbol{\eta}, \underbrace{0, \ldots, 0}_{M - |\mathfrak{m}|})$, (C6) can be rewritten as

$$\sum_{m \in \mathbb{X}} \frac{\partial r_n}{\partial x_m} \eta_m - \sum_{\alpha=1}^{K_s} (\boldsymbol{c}^\alpha)_n \zeta_\alpha = 0, \tag{C7}$$

where the summation of m is taken over all chemicals in Γ. Finally, by multiplying (C7) with the stoichiometry matrix ν and using the fact that $\boldsymbol{c}^\alpha$ is a kernel vector of ν, we obtain

$$\sum_{n \in \mathbb{E}} \nu_{m', n} \sum_{m \in \mathbb{X}} \frac{\partial r_n}{\partial x_m} v_m = 0, \tag{C8}$$

or, equivalently,

$$\sum_{m \in \mathbb{X}} J_{m', m} v_m = 0. \tag{C9}$$

Thus, we have proved that $\det \mathbf{A}_{\Gamma_s} = 0$ is associated with the null vector $\boldsymbol{v}$ of the Jacobian matrix J, whose support is inside chemicals in Γ_s. Thus, (C1) is proved.

A similar argument cannot be applied into a bifurcation associated with $\det \mathbf{A}_{\bar{\Gamma}_s} = 0$: While null vectors of J associated with $\det \mathbf{A}_{\Gamma_s} = 0$ do not have support on chemicals in $\bar{\Gamma}_s$, those associated with $\det \mathbf{A}_{\bar{\Gamma}_s} = 0$ generally have support on both chemicals in $\bar{\Gamma}_s$ and those in Γ_s This difference comes from the nonsymmetric structure of the matrix $\mathbf{A}$ in (B3); while columns associated with chemicals and kernels in Γ_s do not have support on reactions in $\bar{\Gamma}_s$ (see zero entries in the lower-left block in (B3)), those associated with $\bar{\Gamma}_s$ generally have support on both reactions in $\bar{\Gamma}_s$ and those in Γ_s (see nonzero entries in the upper-right block in (B3)).

The discussion in this section can be generalized straightforwardly into a network with multiple buffering structures. The result is summarized as follows: *when the determinant factor of a particular determinant structure becomes zero, the corresponding null vector $\boldsymbol{v}$ of J does not have support inside the minimal buffering structure containing the determinant structure.* This implies that the bifurcation behavior is observed only inside the minimal buffering structure.

Appendix D: Parameters used in Fig. 3 of the main text

The dynamics of the hypothetical example in the main text is given by the following ODEs,

$$
\begin{aligned}
\dot{x}_A &= k_1 - k_2 x_{\mathrm{A}} + k_3 x_{\mathrm{B}} \left(1 + \frac{k_{3,\mathrm{A}} x_{\mathrm{A}}^2}{x_{\mathrm{A}}^2 + 5} \right) \\
\dot{x}_B &= k_2 x_{\mathrm{A}} - k_3 x_{\mathrm{B}} \left(1 + \frac{k_{3,\mathrm{A}} x_{\mathrm{A}}^2}{x_{\mathrm{A}}^2 + 5} \right) - k_4 x_{\mathrm{B}} \left(1 + \frac{k_{4,\mathrm{C}} x_{\mathrm{C}}^2}{x_{\mathrm{C}}^2 + 5} \right) \\
\dot{x}_C &= k_4 x_{\mathrm{B}} \left(1 + \frac{k_{4,\mathrm{C}} x_{\mathrm{C}}^2}{x_{\mathrm{C}}^2 + 5} \right) - k_5 x_{\mathrm{C}} \left(1 + \frac{k_{5,\mathrm{B}} x_{\mathrm{B}}^2}{x_{\mathrm{B}}^2 + 5} \right).
\end{aligned}
\tag{D1}
$$

In Fig.3 of the main text, we used the following parameters. For Fig. 3 (a), $\vec{k} = (80, 85, 20, 46, 43)$ and $(k_{3,\mathrm{A}}, k_{4,\mathrm{C}}) = (5, 70)$. For Fig. 3 (b-1), $\vec{k} = (7, 54, 8, 25, 40)$ and $(k_{4,\mathrm{C}}, k_{5,\mathrm{B}}) = (5, 5)$. For Fig. 3 (b-2), $\vec{k} = (7, 54, 8, 25, 40)$, $(k_{3,\mathrm{A}}, k_{4,\mathrm{C}}) = (99.9, 5)$.

Appendix E: Structural bifurcation analysis for the E. coli network

1. Reaction list for the E. coli

The central carbon metabolism of the E. coli in the main text consists of the following reactions:

1: Glucose + PEP → G6P + PYR.
2: G6P ← F6P.
3: F6P → G6P.
4: F6P → F1,6P.
5: F1,6P → G3P + DHAP.
6: DHAP → G3P.
7: G3P → 3PG.
8: 3PG → PEP.
9: PEP → 3PG.
10: PEP → PYR.
11: PYR → PEP.
12: PYR → AcCoA + CO2.
13: G6P → 6PG.
14: 6PG → Ru5P + CO2.
15: Ru5P → X5P.
16: Ru5P → R5P.
17: X5P + R5P → G3P + S7P.
18: G3P + S7P → X5P + R5P.
19: G3P + S7P → F6P + E4P.
20: F6P + E4P → G3P + S7P.
21: X5P + E4P → F6P + G3P.
22: F6P + G3P → X5P + E4P.
23: AcCoA + → CIT.
24: CIT → ICT.
25: ICT → 2-KG + CO2.
26: 2-KG → SUC + CO2.
27: SUC → FUM.
28: FUM → MAL.
29: MAL → OAA.
30: OAA → MAL.
31: PEP + CO2 → OAA.
32: OAA → PEP + CO2.
33: MAL → PYR + CO2.
34: ICT → SUC + Glyoxylate.
35: Glyoxylate + AcCoA → MAL.
36: 6PG → G3P + PYR.
37: AcCoA → Acetate.
38: PYR → Lactate.
39: AcCoA → Ethanol.
40: R5P → (output).
41: OAA → (output).
42: CO2 → (output).
43: (input) → Glucose.
44: Acetate → (output).
45: Lactate → (output).
46: Ethanol → (output).

2. Buffering structures in the E. coli network

Assuming that each reaction rate function depends on its substrate concentrations, we find 17 different buffering structures in the E. coli system [6]. The inclusion relation between them is summarized in Fig. 5. For each box in Fig. 5, the set of chemicals and reactions (indicated by numbers) in the box plus those in its downward boxes gives a buffering structure. In other words, the set of chemicals and reactions in each box gives a sub-network, which is a buffering structure with subtraction of its inner buffering structures, namely a determinant structure. We remark that, in Fig. 5, while a box without emanating arrows from it, such as ({Glucose}, {1}), corresponds to a buffering structure, a box with emanating arrows from it, such as ({R5P}, {40}), itself is not a buffering structure. The determinant det $\mathbf{A}$ are factorized according to these 17 determinant structures.

We write down explicitly the 17 buffering structures:

$$\mathbf{A} =$$

FIG. 9: The detailed expression of the matrix $\mathbf{A}$ of the E. coli network.

$\Gamma_1 = (\{\text{Glucose}\}, \{1\})$.
$\Gamma_2 = (\{\text{3PG}\}, \{8\})$
$\Gamma_3 = (\{\text{CIT}\}, \{24\})$,
$\Gamma_4 = (\{\text{2-KG}\}, \{26\})$,
$\Gamma_5 = (\{\text{SUC}\}, \{27\})$,
$\Gamma_6 = (\{\text{FUM}\}, \{28\})$,
$\Gamma_7 = (\{\text{Glyoxylate}\}, \{35\})$,
$\Gamma_8 = (\{\text{Acetate}\}, \{44\})$,
$\Gamma_9 = (\{\text{Lactate}\}, \{45\})$,
$\Gamma_{10} = (\{\text{Ethanol}\}, \{46\})$,
$\Gamma_{11} = (\{\text{Glucose}, \text{PEP}, \text{3PG}, \text{PYR}, \text{AcCoA}, \text{OAA}, \text{CIT}, \text{ICT}, \text{2-KG}, \text{SUC}, \text{FUM}, \text{MAL}, \text{CO2}, \text{Glyoxylate}, \text{Acetate}, \text{Lactate}, \text{Ethanol}\}, \{1, 8, 9, 10, 11, 12, 23, 24, 25, 26, 27, 28, 29, 30, 31, 32, 33, 34, 35, 37, 38, 39, 41, 42, 44, 45, 46\})$,
$\Gamma_{12} = (\{\text{X5P}, \text{S7P}, \text{E4P}\}, \{17, 18, 19, 20, 21\})$,
$\Gamma_{13} = (\{\text{G3P}, \text{X5P}, \text{S7P}, \text{E4P}\}, \{7, 17, 18, 19, 20, 21, 22\})$
$\Gamma_{14} = (\{\text{X5P}, \text{R5P}, \text{S7P}, \text{E4P}\}, \{17, 18, 19, 20, 21, 40\})$,

$\Gamma_{15} = (\{\text{F1}, \text{6P}\}, \{5\})$,
$\Gamma_{16} = (\{\text{DHAP}\}, \{6\})$,
$\Gamma_{17} = (\{\text{Glucose}, \text{PEP}, \text{G6P}, \text{F6P}, \text{F1}, \text{6P}, \text{DHAP}, \text{G3P}, \text{3PG}, \text{PYR}, \text{6PG}, \text{Ru5P}, \text{X5P}, \text{R5P}, \text{S7P}, \text{E4P}, \text{AcCoA}, \text{OAA}, \text{CIT}, \text{ICT}, \text{2-KG}, \text{SUC}, \text{FUM}, \text{MAL}, \text{CO2}, \text{Glyoxylate}, \text{Acetate}, \text{Lactate}, \text{Ethanol}\}, \{1, 2, 3, 4, 5, 6, 7, 8, 9, 10, 11, 12, 13, 14, 15, 16, 17, 18, 19, 20, 21, 22, 23, 24, 25, 26, 27, 28, 29, 30, 31, 32, 33, 34, 35, 36, 37, 38, 39, 40, 41, 42, 44, 45, 46\})$.

3. Structural bifurcation analysis for the E. coli network

For the E. coli network, we construct the matrix $\mathbf{A}$. The inclusion relation of the 17 buffering structures shown in Fig. 5 implies that, after permutation of the indices, the matrix $\mathbf{A}$ can be written as shown in Fig. 9.

In the matrix $\mathbf{A}$ in Fig. 9, the column indices (28 chemicals and 18 kernel vectors) are ordered as follows (from left to right):

$$\{\text{Glucose}, \text{3PG}, \boldsymbol{c}_1, \text{CIT}, 2-\text{KG}, \text{SUC}, \text{FUM}, \text{Glyoxylate}, \text{Acetate}, \text{Lactate}, \text{Ethanol}, \text{PEP}, \text{PYR}, \text{AcCoA}, \text{OAA}, \text{CIT},$$
$$, \text{MAL}, \text{CO2}, \boldsymbol{c}_2, \boldsymbol{c}_3, \boldsymbol{c}_4, \boldsymbol{c}_5, \boldsymbol{c}_6, \boldsymbol{c}_7, \boldsymbol{c}_8, \boldsymbol{c}_9, \boldsymbol{c}_{10}, \text{F1}, \text{6P}, \text{DHAP}, \text{G3P}, \text{X5P}, \text{S7P}, \text{E4P}, \boldsymbol{c}_{11}, \boldsymbol{c}_{12}, \boldsymbol{c}_{13}, \text{R5P}, \text{G6P}, \text{F6P}, \text{6PG},$$
$$\text{Ru5P}, \boldsymbol{c}_{14}, \boldsymbol{c}_{15}, \boldsymbol{c}_{16}, \boldsymbol{c}_{17}, \boldsymbol{c}_{18}\}, \tag{E1}$$

and the row indices (46 reactions) are ordered as follows (from top to bottom):

$$\{1, 2, 3, 4, 5, 6, 7, 8, 9, 10, 11, 12, 13, 14, 15, 16, 17, 18, 19, 20, 21, 22, 23, 24, 25, 26, 27, 28, 29, 36, 30, 31, 32, 33, 34, 35,$$
$$37, 38, 39, 40, 41, 42, 43, 44, 45, 46\}. \tag{E2}$$

Each r in Fig. 9 represents the corresponding $r_{n,m}$.

The overall constant of $\det \mathbf{A}$, which depends on normalization of kernel vectors of ν in $\mathbf{A}$, is irrelevant for

our discussion. Up to a constant factor, the determinant $\det \mathbf{A}$ is factorized as

$$
\begin{aligned}
\det \mathbf{A} = {} & r_{1,\text{Glucose}} \times r_{5,\text{F1,6P}} \times r_{6,\text{DHAP}} \times r_{8,\text{3PG}} \\
& \times r_{44,\text{Acetate}} \times r_{45,\text{Lactate}} \times r_{46,\text{Ethanol}} \times r_{24,\text{CIT}} \\
& \times r_{26,\text{2-KG}} \times r_{27,\text{SUC}} \times r_{28,\text{FUM}} \times r_{35,\text{Glyoxylate}} \\
& \times r_{7,\text{G3P}} \times r_{40,\text{R5P}} \\
& \times (r_{17,\text{X5P}} r_{19,\text{S7P}} r_{21,\text{E4P}} + r_{18,\text{S7P}} r_{20,\text{E4P}} r_{21,\text{X5P}}) \\
& \times \det \mathbf{A}_{\Gamma'} \times \det \mathbf{A}_{\Gamma''}
\end{aligned}
$$

$$(E3)$$

Here, $r_{n,m} = \frac{\partial r_n}{\partial x_m}\big|_{\boldsymbol{x}=\boldsymbol{x}^*}$. Each of the 17 factors in (E3) is associated with a subnetwork in Fig. 5. Here, the first three lines are the factors $\det \mathbf{A}_{\Gamma_s}$ ($s = 1,3,4,6,9,10,11,12,13,15,16,17$), each of which is associated with a buffering (determinant) structure Γ_s with a single chemical. In the fourth and fifth lines, $r_{7,\text{G3P}}$, $r_{40,\text{R5P}}$, and the factor inside (...) are associated with the three determinant structures, $(\{\text{G3P}\},\{7\})$, $(\{\text{R5P}\},\{40\})$, and $\Gamma_{12} = (\{\text{X5P}, \text{S7P}, \text{E4P}\}, \{17,18,19,20,21,22\})$ in Fig 5, respectively. The factor $\det \mathbf{A}_{\Gamma'}$ in the last line of (E3) is associated with the subnetwork $\Gamma' = (\{\text{G6P}, \text{F6P}, \text{6PG}, \text{Ru5P}\}, \{2,3,4,13,14,15,16,36,43\})$ (the green box in Fig. 5) and given by

$$
\begin{aligned}
\det \mathbf{A}_{\Gamma'} = {} & r_{2,\text{G6P}} r_{4,\text{F6P}} \left(r_{15,\text{Ru5P}} + r_{16,\text{Ru5P}}\right) \left(r_{14,\text{6PG}} + r_{36,\text{6PG}}\right) \\
& + r_{13,\text{G6P}} \Big(r_{4,\text{F6P}} \left(r_{15,\text{Ru5P}} + r_{16,\text{Ru5P}}\right) \left(r_{14,\text{6PG}} + r_{36,\text{6PG}}\right) \\
& + r_{3,\text{F6P}} \big(r_{14,\text{6PG}} r_{16,\text{Ru5P}} + \left(r_{15,\text{Ru5P}} + r_{16,\text{Ru5P}}\right) r_{36,\text{6PG}}\big) \Big).
\end{aligned}
$$

$$(E4)$$

The last factor $\det \mathbf{A}_{\Gamma''}$ in (E3) is associated with the subnetwork $\Gamma'' = (\{\text{PEP}, \text{PYR}, \text{AcCOA}, \text{OAA}, \text{ICT}, \text{MAL}, \text{CO2}\}, \{10,11,12,23,25,29,30,31,32,33,34,37,38,39,41,42\})$ (the red box in Fig. 5) and given by

$$
\begin{aligned}
\det \mathbf{A}_{\Gamma''} = {} & r_{10,\text{PEP}}(r_{38,\text{PYR}}(r_{23,\text{OAA}}(r_{37,\text{AcCoA}} + r_{39,\text{AcCoA}})(r_{25,\text{ICT}}(2r_{29,\text{MAL}}r_{31,\text{CO2}} \\
& + r_{33,\text{MAL}}(2r_{31,\text{CO2}} - r_{42,\text{CO2}}) + r_{34,\text{ICT}}(r_{33,\text{MAL}}(r_{31,\text{CO2}} - r_{42,\text{CO2}}) + r_{29,\text{MAL}}(r_{31,\text{CO2}} + r_{42,\text{CO2}}))) \\
& - (r_{23,\text{AcCoA}}(r_{25,\text{ICT}} + 2r_{34,\text{ICT}}) + (r_{25,\text{ICT}} + r_{34,\text{ICT}})(r_{37,\text{AcCoA}} + r_{39,\text{AcCoA}}))(r_{29,\text{MAL}}(r_{31,\text{CO2}}r_{41,\text{OAA}} \\
& + (r_{32,\text{OAA}} + r_{41,\text{OAA}})r_{42,\text{CO2}}) + r_{33,\text{MAL}}(r_{31,\text{CO2}}r_{41,\text{OAA}} + (r_{30,\text{OAA}} + r_{32,\text{OAA}} + r_{41,\text{OAA}})r_{42,\text{CO2}}))) \\
& + r_{12,\text{PYR}}(-(r_{25,\text{ICT}} + r_{34,\text{ICT}})(r_{37,\text{AcCoA}} + r_{39,\text{AcCoA}})(r_{29,\text{MAL}}(2r_{31,\text{CO2}}r_{41,\text{OAA}} \\
& + (r_{32,\text{OAA}} + r_{41,\text{OAA}})r_{42,\text{CO2}}) + r_{33,\text{MAL}}(2r_{31,\text{CO2}}r_{41,\text{OAA}} + (r_{30,\text{OAA}} + r_{32,\text{OAA}} + r_{41,\text{OAA}})r_{42,\text{CO2}})) \\
& + r_{23,\text{OAA}}(r_{37,\text{AcCoA}} + r_{39,\text{AcCoA}})(r_{25,\text{ICT}}(2r_{29,\text{MAL}}r_{31,\text{CO2}} + r_{33,\text{MAL}}(2r_{31,\text{CO2}} - r_{42,\text{CO2}})) \\
& + r_{34,\text{ICT}}(r_{33,\text{MAL}}(2r_{31,\text{CO2}} - r_{42,\text{CO2}}) + r_{29,\text{MAL}}(2r_{31,\text{CO2}} + r_{42,\text{CO2}}))) \\
& - r_{23,\text{AcCoA}}(r_{25,\text{ICT}}(r_{33,\text{MAL}}(4r_{31,\text{CO2}}r_{41,\text{OAA}} + (r_{30,\text{OAA}} \\
& + r_{32,\text{OAA}})r_{42,\text{CO2}}) + r_{29,\text{MAL}}(4r_{31,\text{CO2}}r_{41,\text{OAA}} + (r_{32,\text{OAA}} + r_{41,\text{OAA}})r_{42,\text{CO2}})) \\
& + r_{34,\text{ICT}}(r_{33,\text{MAL}}(4r_{31,\text{CO2}}r_{41,\text{OAA}} + (r_{30,\text{OAA}} + r_{32,\text{OAA}})r_{42,\text{CO2}}) \\
& + r_{29,\text{MAL}}(4r_{31,\text{CO2}}r_{41,\text{OAA}} + (r_{32,\text{OAA}} + 2r_{41,\text{OAA}})r_{42,\text{CO2}})))))) \\
& - r_{31,\text{PEP}}(-r_{11,\text{PYR}}(r_{29,\text{MAL}} + r_{33,\text{MAL}})(r_{23,\text{OAA}}r_{34,\text{ICT}}(r_{37,\text{AcCoA}} + r_{39,\text{AcCoA}}) \\
& - (r_{23,\text{AcCoA}}(r_{25,\text{ICT}} + 2r_{34,\text{ICT}}) + (r_{25,\text{ICT}} + r_{34,\text{ICT}})(r_{37,\text{AcCoA}} + r_{39,\text{AcCoA}}))r_{41,\text{OAA}}) \\
& + r_{38,\text{PYR}}(r_{23,\text{AcCoA}}(r_{25,\text{ICT}} + 2r_{34,\text{ICT}})(r_{30,\text{OAA}}r_{33,\text{MAL}} + (r_{29,\text{MAL}} + r_{33,\text{MAL}})r_{41,\text{OAA}}) \\
& + (r_{37,\text{AcCoA}} + r_{39,\text{AcCoA}})(r_{23,\text{OAA}}(r_{25,\text{ICT}}r_{33,\text{MAL}} + (r_{33,\text{MAL}} - r_{29,\text{MAL}})r_{34,\text{ICT}}) \\
& + (r_{25,\text{ICT}} + r_{34,\text{ICT}})(r_{30,\text{OAA}}r_{33,\text{MAL}} + (r_{29,\text{MAL}} + r_{33,\text{MAL}})r_{41,\text{OAA}}))) \\
& + r_{12,\text{PYR}}(r_{23,\text{AcCoA}}(r_{25,\text{ICT}}(r_{30,\text{OAA}}r_{33,\text{MAL}} \\
& + r_{29,\text{MAL}}r_{41,\text{OAA}}) + r_{34,\text{ICT}}(r_{30,\text{OAA}}r_{33,\text{MAL}} + 2r_{29,\text{MAL}}r_{41,\text{OAA}})) + (r_{37,\text{AcCoA}} \\
& + r_{39,\text{AcCoA}})(r_{23,\text{OAA}}(r_{25,\text{ICT}}r_{33,\text{MAL}} + (r_{33,\text{MAL}} - r_{29,\text{MAL}})r_{34,\text{ICT}}) \\
& + (r_{25,\text{ICT}} + r_{34,\text{ICT}})(r_{30,\text{OAA}}r_{33,\text{MAL}} + (r_{29,\text{MAL}} + r_{33,\text{MAL}})r_{41,\text{OAA}})))r_{42,\text{CO2}}.
\end{aligned}
$$

$$(E5)$$

Since $r_{n,m} > 0$, we see that, among the 17 factors in (E3), only the last factor $\det \mathbf{A}_{\Gamma''}$ contains both of plus and minus signs. Therefore, if this system exhibits a steady-state bifurcation (under parameter change), it should be the subnetwork Γ'' whose determinant changes its sign at the bifurcation point.

4. Numerical analysis

In the discussion so far, we have not assumed any specific kinetics for reaction rates. To numerically demonstrate bifurcation behaviors in the E. coli system, we first consider the case that all the reactions obey the mass-action kinetics with reaction rate constant k_n ($n = 1,\ldots,47$). In this case, we found that, for any parameter choices, the E. coli system has either a single stable solution or a blow up solution, and no steady-state bi-

furcations were observed. We also performed the same analysis in the case of the Michaelis-Menten kinetics, and again no bifurcations were observed.

In order to demonstrate bifurcation behaviors, we next consider the case that the reaction $11 : \text{PYR} \rightarrow \text{PEP}$ is positively regulated by PEP. Specifically, we modified the rate of reaction 11 from $r_{11} = k_{11} x_{\text{PYR}}$ into

$$r_{11} = k_{11} x_{\text{PYR}} \left(1 + k_{11,PEP} \frac{x_{\text{PEP}}^2}{x_{\text{PEP}}^2 + K} \right) \qquad (E6)$$

where $k_{11,\text{PEP}}$ represents the strength of the regulation. All reactions except reaction 11 obey the mass-action kinetics as before.

We remark that the regulation from PEP to reaction 11 does not change the buffering structures in Appendix E 2 since adding this regulation does not ruin the condition of output-completeness. This is generally the case, if an additional regulation is within a buffering structure Γ_s, i.e. from a chemical in Γ_s to a reaction in Γ_s. Thus, the inclusion relation of buffering structures shown in Fig. 5 is also intact under the modification (E6) of the kinetics.

As explained previously, only bifurcations associated with Γ'' (the red box in Fig 5) are possible for this system. The inducing parameters are then given by parameters associated with reactions in the green and red boxes in Fig 5. As a candidate bifurcation parameter, we choose the parameter $k_{11,PEP}$, which is associated with reaction 11 and is an inducing parameter for Γ''. The reaction rate constants of the mass-action kinetics were set as

$$
\begin{aligned}
(k_1, \dots, k_{47}) = (&18.9, 55.9, 20.5, 5.17, 8.14, 107, 15.7, 2.38, 32, 3.08, \\
&38.8, 471, 7.54, 1.28, 24.4, 84.9, 23.1, 1.64, 90.6, 132, \\
&65, 47, 237, 1.19, 11.7, 1.80, 98.5, 27, 1090, 3.15, \\
&484, 1.44, 543, 12.2, 20, 89.5, 2.98, 7.23, 48.9, 2.96, \\
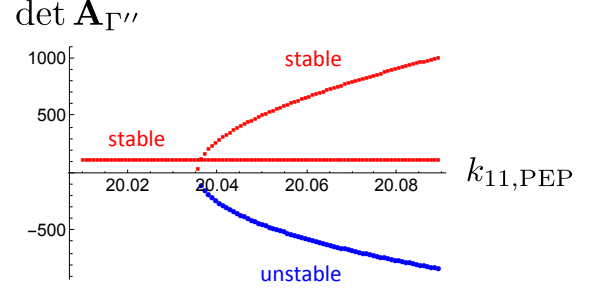&21.6, 37.6, 85, 131, 28.2, 2.37). \qquad (E7)
\end{aligned}
$$

FIG. 10: $\det \mathbf{A}_{\Gamma''}$ versus $k_{11,PEP}$. The red curves (in the region $\det \mathbf{A}_{\Gamma''} > 0$) correspond to two stable solutions, and the blue curve (in the region $\det \mathbf{A}_{\Gamma''} < 0$)corresponds to an unstable solution.

Fig. 10 shows the numerical result for $\det \mathbf{A}_{\Gamma''}$ versus $k_{11,PEP}$. For large $k_{11,PEP}$, there are two stable solutions (red curves) and one unstable solution (blue curve). As $k_{11,PEP}$ is decreased, the magnitudes of $\det \mathbf{A}_{\Gamma''}$ for a stable and unstable solutions decreases and eventually approach zero. Thus, the parameter $k_{11,PEP}$, which is one of the inducing parameters for Γ'', actually induces a bifurcation associated with Γ''.

The bifurcating chemicals for Γ'' are those in the blue and red boxes. Fig. 7 shows the numerical results for the steady-state concentrations versus the parameter $k_{11,\text{PEP}}$. We see that saddle-node bifurcations are observed only for the bifurcating chemicals.

[1] Ogata, H., Goto, S., Sato, K., Fujibuchi, W., Bono, H., Kanehisa, M. (1999). KEGG: Kyoto encyclopedia of genes and genomes. Nucleic acids research, 27(1), 29-34.
[2] Joshi-Tope, G., Gillespie, M., Vastrik, I., D'Eustachio, P., Schmidt, E., de Bono, B., Stein, L. (2005). Reactome: a knowledgebase of biological pathways. Nucleic acids research, 33(suppl 1), D428-D432.
[3] Karp, P. D., Ouzounis, C. A., Moore-Kochlacs, C., Goldovsky, L., Kaipa, P., Ahrén, D., López-Bigas, N. (2005). Expansion of the BioCyc collection of pathway/genome databases to 160 genomes. Nucleic acids research, 33(19), 6083-6089.
[4] Ishii, N., Nakahigashi, K., Baba, T., Robert, M., Soga, T., Kanai, A., Tomita, M. (2007). Multiple high-throughput analyses monitor the response of E. coli to perturbations. Science, 316(5824), 593-597.
[5] Mochizuki, A., Fiedler, B.,Journal of theoretical biology, 367, 189-202 (2015).
[6] Okada T. and Mochizuki A., Phys. Rev. Lett. **117**.4 (2016), 048101.
[7] Okada T. and Mochizuki A., Phys. Rev. E 96, 022322 (2017).

[8] Ozbudak, Ertugrul M., et al. Nature 427.6976: 737-740 (2004).
[9] See Supplemental Material at [URL will be inserted by publisher] for the generalization to networks with conserved concentrations.
[10] J. Carr, "Applications of center manifold theory", Springer (1981).
[11] A.A. Andronov, E.A. Leontovich, I.I. Gordon, A.G. Maier, "Theory of bifurcations of dynamical systems on a plane", Israel Program Sci. Transl. (1971). (In Russian)
[12] V.I. Arnol'd, "Geometrical methods in the theory of ordinary differential equations" , Grundlehren math. Wiss., **250**, Springer (1983). (In Russian)
[13] J. Guckenheimer and Ph. Holmes, "Nonlinear oscillations, dynamical systems and bifurcations of vector fields", Springer (1983).
[14] Yu.A. Kuznetsov, "Elements of applied bifurcation theory", Springer (1995).
[15] Warburg, O. Naturwissenschaften, 12(50), 1131-1137. (1924).
[16] Conradi, Carsten, Dietrich Flockerzi, and Jorg Raisch. American Control Conference, 2007. ACC'07. IEEE,

2007.

[17] F. Schlögl, Zeitschrift für Physik A Hadrons and Nuclei 253.2 (1972): 147-161.

[18] M. Feinberg, Arch. Rational Mech. Anal. **132** (1995), pp. 311–370.

[19] M. Feinberg, Arch. Rational Mech. Anal. **132** (1995), pp. 371–406.

[20] G. Craciun and M. Feinberg, SIAM J. Appl. Math. **65** (2005), pp. 1526–1546

[21] G. Craciun and M. Feinberg, SIAM J. Appl. Math. **66** (2006), pp. 1321–1338.

[22] Mincheva, M., & Roussel, M. R. (2007). Journal of mathematical biology, 55(1), 61.

[23] Shinar, G., & Feinberg, M. (2010). Science, 327(5971), 1389-1391

[24] B.D. Aguda and B.L. Clarke, J. Chem. Phys. **87** (1987), pp. 3461–3470.

[25] B.L. Clarke, J. Chem. Phys. **62** (1975), pp. 773–775.

[26] B.L. Clarke, J. Chem. Phys. **62** (1975), pp. 3726–3738.

[27] B.L. Clarke, Adv. Chem. Phys. Wiley, New York, vol 43, pp 1–216.

[28] K. Gatermann, M. Eiswirth, and A. Sensse, J. Symb. Comput. **40** (2005), pp. 1361–1382.

[29] B.L. Clarke and W. Jiang, J. Chem. Phys. **99** (1993), pp. 4464–4476.